



UNIVERSITÀ DEGLI STUDI DI MILANO
FACOLTÀ DI SCIENZE E TECNOLOGIE

CORSO DI LAUREA TRIENNALE IN FISICA

**Devil's staircase and ground states of
long range 1D lattice gas**

Relatore: Prof. Luca Guido Molinari

Correlatore: Dott. Pietro Rotondo

Elaborato di:

Piergiorgio Ratti

Matr. 777613

Codice P.A.C.S.: 05.50.-q

Anno Accademico 2014-2015

Contents

Riassunto	3
Abstract	4
1 Quantum Hall Effects	5
1.1 Introduction	5
1.2 Hall effects	5
1.2.1 Classical Hall effect	5
1.2.2 Quantum Hall effect	6
1.3 Landau levels	7
1.3.1 Symmetric Gauge	10
1.3.2 Landau Gauge	11
1.3.3 Flux quanta and filling factor	11
1.4 Integer Quantum Hall effect	12
1.5 Fractional Quantum Hall effect	12
2 TT hamiltonian	14
2.1 Microscopic model	14
2.2 TT Coulomb matrix element	16
2.3 Momentum target space	17
2.4 Mapping on long-range repulsive lattice gas	19
3 Lattice gas models	22
3.1 Introduction	22
3.2 The Ising model	22
3.2.1 Definition of the model	22
3.2.2 Classification of models	23
3.2.3 Noninteracting spins Ising model: exact solution	23
3.2.4 Nearest-neighbor Ising models: mean field approximation	24
3.2.5 Ferromagnetic nearest-neighbor Ising model: analytical solutions	25
3.2.6 Lattice gas	26
3.3 Ground States	26
3.3.1 Introduction	26
3.3.2 Hubbard ground-states	26
3.3.3 Hubbard algorithm	34
3.4 Phase transitions	34
3.4.1 Devil's staircase	35
Conclusions	39

Riassunto

Nel 1983 R. Tao and D. J. Thouless (TT) proposero un approccio microscopico all'effetto Hall quantistico frazionario (FQHE) [1]. Suggestarono che un sistema bidimensionale di elettroni in campo magnetico intenso forma un cristallo di Wigner [2] monodimensionale nel reticolo del sottospazio delle funzioni d'onda del più basso livello di Landau (LLL). Questo strano cristallo di elettroni era responsabile, a loro parere, della quantizzazione frazionaria della resistività di Hall che si osserva sperimentalmente. Motivarono la loro soluzione sviluppando un metodo Hartree-Fock sulla hamiltoniana in seconda quantizzazione per N elettroni interagenti in campo magnetico descritti con funzioni d'onda del LLL. Tuttavia la loro teoria microscopica fu successivamente abbandonata (da Thouless in prima persona [3]) perché era in conflitto con il celebre "ansatz di Laughlin" [4] per le funzioni d'onda degli stati di effetto Hall con "filling fractions" $\nu = 1/q$ con q dispari.

Nell'elaborato, dopo aver introdotto una descrizione fenomenologica dell'effetto Hall quantistico, della quantizzazione di Landau, e delle teorie fenomenologiche di Laughlin, si rivaluta la teoria di TT, esibendo una analisi esatta della hamiltoniana di interazione degli elettroni sul LLL. Dallo studio potrebbe emergere che i cristalli di Wigner generalizzati giocano un ruolo fondamentale nella teoria dell'effetto Hall, seppur in modo differente rispetto alle previsioni di TT.

Il punto di partenza è l'hamiltoniana in seconda quantizzazione proiettata sulle base delle funzioni di LLL di un sistema bidimensionale a geometria cilindrica (cioè con condizioni periodiche solo in una direzione) di elettroni sottoposti ad interazione coulombiana e posti in campo magnetico costante intenso. L'elemento di matrice di Coulomb è stato calcolato da TT nel loro articolo. Si mostra che, nel limite termodinamico, cioè nel limite in cui la dimensione del sistema è molto maggiore della lunghezza caratteristica del sistema (la lunghezza magnetica), questo elemento di matrice è invariante per traslazioni nello spazio dei numeri quantici delle funzioni LLL. Ciò comporta che l'hamiltoniana nello spazio dei momenti assuma una forma già nota in meccanica statistica: l'hamiltoniana del modello di Bak, cioè una hamiltoniana di "lattice gas" monodimensionale con interazione a lungo raggio repulsiva. Nel terzo capitolo dell'elaborato, dopo aver brevemente discusso i modelli di Ising su reticolo, si analizza l'hamiltoniana di Bak; facendo alcune ipotesi, a cui si assoggetta anche il potenziale coulombiano, sulla struttura analitica del potenziale, è possibile derivare la forma esatta dei ground states (detti ground states di Hubbard) e costruire il diagramma di fase. Quest'ultimo presenta una forma frattale, nota come "Devil's Staircase". Nonostante il potenziale ottenuto calcolando la trasformata di Fourier dell'elemento di matrice di TT non rispetti esattamente le ipotesi richieste dal modello di Bak, la struttura della "Devil's Staircase" ottenuta sembra ben imitare il comportamento a plateau della conduttività di Hall in funzione del campo magnetico, soprattutto per quanto concerne la lunghezza relativa dei plateau.

In conclusione, questa tesi elabora e sviluppa l'idea che il meccanismo microscopico alla base della quantizzazione frazionaria delle "filling fraction" dell'effetto Hall quantistico possa essere dovuto ad un fenomeno collettivo emergente, tipico dei lattice gas con interazione repulsiva a lungo raggio.

Abstract

In 1983 R. Tao and D. J. Thouless (TT) proposed a microscopic approach to fractional quantum Hall effect (FQHE) [1]. They suggested that electrons in a strong magnetic field could form a one dimensional *Wigner crystal* [2] in the lattice *target space* of the lowest Landau Level (LLL). This weird electron crystal was responsible, in their opinion, of the observed experimentally fractional quantization of the Hall resistivity. They motivated their claim with a sloppy Hartree-Fock analysis of the complete second quantization Hamiltonian for N interacting electrons in a magnetic field restricted to the LLL. However their microscopic theory was later abandoned (by Thouless in first person [3]) because it was in conflict with the celebrated *Laughlin's ansatz* [4] for the wave function of the $\nu = 1/q$ odd filling factors Quantum Hall states.

The elaborate, after introducing a phenomenological description of the quantum Hall effect, the quantization of Landau, and phenomenological theories of Laughlin, appreciates the theory of TT, exhibiting an exact analysis of the Hamiltonian of interaction of electrons on LLL. From study it could emerge that the generalized Wigner crystals plays an important role in the theory of the Hall effect, albeit in a different way than forecast in TT.

The starting point is the hamiltonian in second quantization projected on the basis of the functions of LLL of a two-dimensional system with cylindrical geometry (ie with periodic conditions in one direction only) of electrons subjected to Coulomb interaction and placed in a constant high magnetic field. The Coulomb matrix element was calculated by TT in their article. It shows that, in the thermodynamic limit, that is, in the limit in which the system size is much greater than the characteristic length of the system (the magnetic length), this matrix element is invariant to translations in space of the quantum numbers of the functions LLL. This means that the hamiltonian in momentum space presents a form already known in statistical mechanics: the hamiltonian of Bak's model, that is an hamiltonian of one-dimensional long-range repulsive "lattice gas". In third chapter of the paper, after briefly discussed Ising's models on lattice, we analyze the Bak's hamiltonian; making some assumptions, to which it also subjects the Coulomb potential, on the analytical structure of the potential, it is possible to derive the exact shape of the ground states (called Hubbard's ground states) and construct the phase diagram, that has a fractal shape, known as "Devil's Staircase". Despite the potential obtained by calculating the Fourier transform of the array element of TT does not meet exactly the assumptions required by the Bak's model, the structure of the "Devil's Staircase" obtained seems well to imitate the behavior of the conductivity plateau of Hall in function of the field magnetic, especially as regards the relative length of the plateau.

In conclusion, this thesis elaborates and develops the idea that the microscopic mechanism behind the fractional quantization of "filling fraction" of quantum Hall effect may be due to a collective phenomenon emerging, typical of the lattice gas with long-range repulsive interaction.

Chapter 1

Quantum Hall Effects

1.1 Introduction

The quantum Hall (QH) effect is one of the most noteworthy macroscopic quantum phenomena discovered in the last century. The integer QH effect was discovered in 1980 by K. von Klitzing, a century after the discovery of the classical Hall effect, for which he received the Nobel prize in 1985. The fractional QH effect was discovered in 1982 by D. Tsui, H. Stormer and A.C.Gossard. In 1983 B. Laughlin proposed an ansatz to understand the phenomenon. B. Laughlin, D. Tsui and H. Stormer received the Nobel prize in 1998.

QH effects are so special in condensed matter physics that they are deeply connected with fundamental principles of physics. It is a rare opportunity to enjoy the interplay between condensed matter physics and particle physics. Moreover, QH effects are an open field of research. Many fancy ideas appear: composite particle (boson or fermion), skyrmions, pseudospins and topological solitons are examples of them.

This chapter is intended to give a self-contained introduction to principal concepts in QH effects, starting from phenomenological approach. The reader may profitably consult [\[5\]](#) [\[6\]](#).

1.2 Hall effects

1.2.1 Classical Hall effect

Edwin Hall discovered in 1879 [\[7\]](#), while he was working on his doctoral degree, that in a conductor travelled by electric current and immersed in a magnetic field perpendicular to the current, a voltage difference (the Hall voltage) appears across the electrical conductor, transverse to the electric current.

Classically, electrons moving with velocity \mathbf{v} in an xy plane (2D-system) in magnetic field \mathbf{B} , obey the equation of motion

$$m_e \dot{\mathbf{v}} = -q_e (\mathbf{E} + \mathbf{v} \times \mathbf{B}) \quad (1.1)$$

where m_e is the electron mass and q_e is the electron charge. It implies that $\mathbf{E} = -\mathbf{v} \times \mathbf{B}$, for static current, i.e. $\dot{\mathbf{v}} = 0$. The current density is $\mathbf{J} = -q_e \rho_0 \mathbf{v}$ in a homogeneous electron gas with areal density ρ_0 . It means that

$$J_x = \frac{q_e \rho_0}{B_\perp} E_y, \quad J_y = -\frac{q_e \rho_0}{B_\perp} E_x \quad (1.2)$$

with $B_\perp := -B_z > 0$. The current \mathbf{J} flows in a direction perpendicular to the electrical field \mathbf{E} .

We take the electric field in the y axis; then $E_x = 0$ and $E_y \neq 0$. It follows that the classical Hall resistivity ρ_{xy} is

$$\rho_{xy} = -\rho_{yx} = \frac{E_y}{J_x} = \frac{B_\perp}{q_e \rho_0} = \frac{2\pi\hbar}{q_e^2} \frac{1}{\nu} \quad (1.3)$$

with

$$\nu := \frac{2\pi\hbar\rho_0}{q_e B_\perp} \quad (1.4)$$

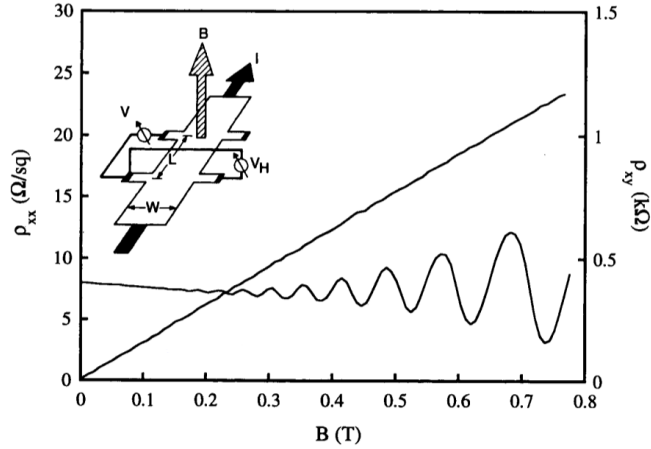


Figure 1.1: Classic Hall effect: low temperature and moderately low B . The insert shows the measurement geometry. The voltages V_x and V_y are respectively measured along and perpendicular. ρ_{xx} is the resistivity across the square. $\rho_{xy} = V_y/I$ is the Hall resistivity. Image taken from [8].

while the diagonal resistivity ρ_{xx} is

$$\rho_{xx} = \rho_{yy} = \frac{E_x}{J_x} = 0 \quad (1.5)$$

1.2.2 Quantum Hall effect

The classical Hall resistivity is a linear function of the perpendicular magnetic field B_\perp for fixed density ρ_0 . It is a common knowledge that the resistivity depends sensitively on details of a sample such as its composition, geometry and impurities. Experimental results are strikingly different, though they are obtained in dirty solid-state samples. The resistivity is insensitive to details of samples at particular values of parameter ν , where the Hall resistivity ρ_{xy} is quantized and develops a series of plateaux, and the diagonal resistivity ρ_{xx} shows a series of dips. This is known as QH effect. The number of observed Hall plateaux increases as the sample becomes purer.

The integer QH effect (IQHE), i.e. at $\nu \in \mathbb{N}$, was discovered by von Klitzing [9] in 1980 in a 2D electron gas at low temperature, a century after the discovery of the Hall effect. The discovery was preceded by a theoretical suggestion due to Ando and an experimental indication due to Kawaji, but no one seems to have foreseen the exact quantization of the Hall conductivity. The fractional QH effect (FQHE), i.e. at $\nu = p/q$ with integer p and odd integer q , was discovered by Tsui, Stormer and Gossard [10] in 1982. While the IQHE can be understood within an independent electron theory of a disordered system, the FQHE is based on strong electron correlations. Both effects are found in GaAs/Ge_xGa_{1-x}As heterostructures of silicon field-effect transistors when a magnetic field B is applied perpendicularly to the two-dimensional electron liquid.

While the actual experimental data are affected by the thermal motion, theoretically it is believed that in the zero temperature limit, the Hall resistivity is given by

$$\rho_{yx} = \frac{1}{\nu} R_K \quad \text{with} \quad R_K := \frac{2\pi\hbar}{q_e^2} = 25812.8074434(84)\Omega \quad (1.6)$$

Because its precise measurement is possible rather easily in QH systems, since 1990 this has been used as the standard resistance with a definite choice of R_K , called the von Klitzing constant.

How can we measure QH effects? The Hall resistivity ρ_{yx} and the diagonal resistivity ρ_{xx} are determined in a rectangular sample by feeding a constant current $J_{tot} = J_x W$ along the x axis and measuring the voltage V_y perpendicular to it (see Figure 1.4). It is arranged so that no current flows in the y direction, $J_y = 0$. The electric field reads

$$E_x = -\rho_{xx} J_x = -\rho_{xx} \frac{J_{tot}}{W}, \quad E_y = -\rho_{yx} J_x = \rho_{yx} \frac{J_{tot}}{W} \quad (1.7)$$

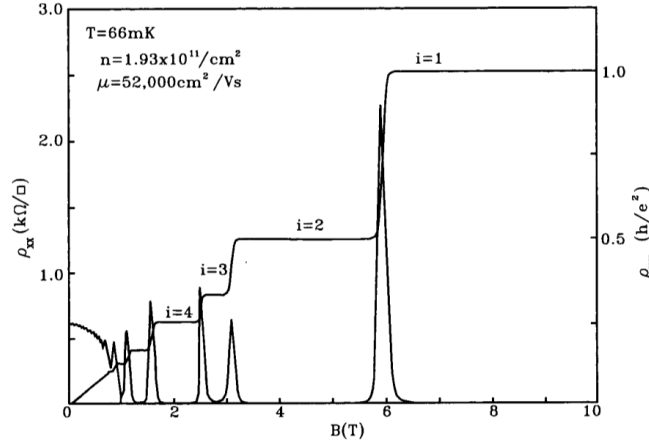


Figure 1.2: The integer QH effect (IQHE). In a classical electron gas the Hall resistivity ρ_{yx} is proportional to the magnetic field B_{\perp} . It works well in weak magnetic field ($B_{\perp} \lesssim 0.3 T$) approximation. However, the Hall resistivity ρ_{xy} shows a stair case in an actual sample, with the plateau crossing the classical line at $\nu = 1, 2, 3, \dots$. The diagonal resistivity ρ_{xx} vanishing at these points. Image taken from [8].

where $E_y = V_y/W$ and $E_x = V_x/L$. It follows that

$$\rho_{xy} = \frac{V_y}{J_{tot}}, \quad \rho_{xx} = -\frac{WV_x}{LJ_{tot}} \quad (1.8)$$

The Hall resistivity ρ_{xy} depends only on the current J_{tot} and the voltage V_y . Hence, it can be determined very accurately. They take peculiar values,

$$\rho_{xy} = \frac{R_K}{\nu}, \quad \rho_{xx} = 0 \quad (1.9)$$

in the QH state at ν . In weak magnetic field, the Hall resistivity is described well by the classical theory, $\rho_{xy} = B_{\perp}/q_e\rho_0$, which is used experimentally to determine the electron density ρ_0 of a sample.

1.3 Landau levels

Before going to explain microscopic QH theories, we have to introduce the quantum description of an electron (or a charge particle) in electromagnetic field in two-dimensional system [6, 11, 12]. We ignore spin degree of freedom in our treatise, so we start from the hamiltonian

$$H_{EM} = \frac{(\mathbf{p} - q_e\mathbf{A})^2}{2m_e} + q_eV \quad (1.10)$$

where \mathbf{p} is the canonical momentum operator that satisfies canonical commutation relations $[r_a, p_b] = i\hbar\delta_{a,b}$ and $(V(\mathbf{r}, t), \mathbf{A}(\mathbf{r}, t))$ is the potential of electromagnetic field:

$$\mathbf{E} = -\nabla V - \frac{\partial \mathbf{A}}{\partial t}, \quad \mathbf{B} = \nabla \times \mathbf{A} \quad (1.11)$$

In absence of electromagnetic field, electrons are free particles on (x, y) plane and they are described by plane waves with energy $E_k = \hbar^2\mathbf{k}^2/2m_e$ and wave vector $\mathbf{k} = \frac{2\pi}{L}(n_x, n_y)$.

Before going to obtain particle's wave function we need to discuss gauge invariance for electromagnetic systems. We observe that H_{EM} doesn't depend on electromagnetic field but only on potential. If we fix electromagnetic field, the choice of electromagnetic potential isn't unique:

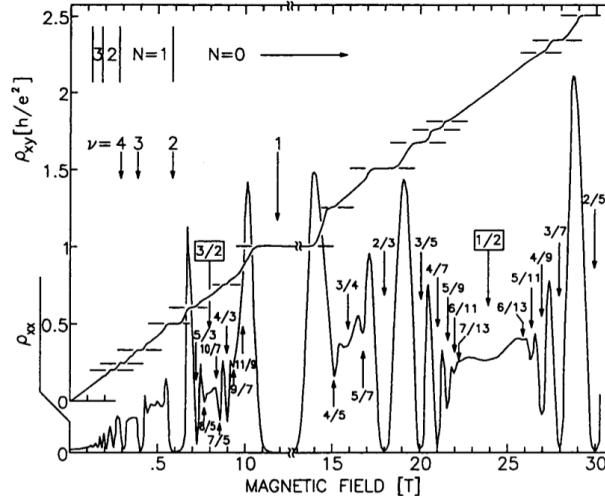


Figure 1.3: The fractional QH effect (FQHE). Many fractional QH states are observed in pure samples. It is easy to identify them by searching for dips in the diagonal resistance ρ_{xx} rather than plateaux in the Hall resistance ρ_{xy} . Image taken from [8].

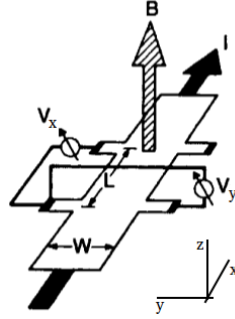


Figure 1.4: Experimental arrangement for measuring the quantum Hall effect.

they are defined less than gradient of an arbitrary function of coordinates and time f (gauge transformation):

$$\mathbf{A}' = \mathbf{A} + \nabla f, \quad V' = V - \frac{\partial f}{\partial t} \quad (1.12)$$

Therefore, a different choice of electromagnetic potential entails different results for wave function of the system. Since this transformation doesn't influence fields, it hasn't to change any quantity that has a physical significance (where there isn't the direct potentials expression). If we define the unitary operator

$$G := \exp \left[\frac{iq_e f}{\hbar} \right] \quad (1.13)$$

it can be verified that the transformation

$$\psi'(\mathbf{r}) := G\psi(\mathbf{r}) \quad (1.14)$$

doesn't change the physics of the system. For example the probability of finding an electron in \mathbf{r} , $|\psi(\mathbf{r})|^2$, keeps unchanged after the transformation. Similarly for $\langle \mathbf{r} \rangle$ and $\langle \mathbf{p} - q_e \mathbf{A} \rangle$. The observable invariance respect to the choice of potentials, names gauge invariance.

Now we want to calculate eigenstates and eigenvalues for the hamiltonian H_{EM} , setting $V = 0$ and $\mathbf{A} = \mathbf{A}(\mathbf{r})$, i.e. we study a particle in homogeneous constant magnetic field $\mathbf{B} = (0, 0, B)$. If we define the gauge invariant momentum $\boldsymbol{\pi}$, the covariant momentum, that correspond to classical generalized momentum¹ $m_e \mathbf{v}$:

$$\boldsymbol{\pi} := m_e \mathbf{v} = \mathbf{p} - q_e \mathbf{A} \quad (1.15)$$

the hamiltonian becomes

$$H_{EM} = \frac{\boldsymbol{\pi}^2}{2m_e} = \frac{1}{2m_e} (\pi_x^2 + \pi_y^2) \quad (1.16)$$

Following commutation relations count for the operators of dynamic momentum components

$$[\pi_x, \pi_y] = i \frac{\hbar}{l_B^2} \quad (1.17)$$

with the magnetic length $l_B := \sqrt{\hbar/q_e B}$, that gives the fundamental scale to the QH system ($B = 10T$ means $l_B \simeq 100\text{\AA}$). We observe that in magnetic field the operators of covariant momentum components don't commute. It means that particle can't have given values of velocity in different directions. Furthermore, using that commutation relation, we can define a creation (increasing) and an annihilation (decreasing) operator, for which $[a, a^\dagger] = 1$,

$$a := \frac{l_B}{\sqrt{2\hbar}} (\pi_x - i\pi_y), \quad a^\dagger := \frac{l_B}{\sqrt{2\hbar}} (\pi_x + i\pi_y) \quad (1.18)$$

The hamiltonian has the same algebraic structure of an harmonic oscillator so

$$H_{EM} = \hbar\omega_c \left(aa^\dagger + \frac{1}{2} \right) \quad (1.19)$$

where $\omega_c := q_e B/m_e$ is the cyclotronic frequency. We know the structure of the spectrum of an harmonic oscillator. The eigenstates of H_{EM} are the same of the number operator $N = a^\dagger a$ that we define $N|n\rangle = n|n\rangle$. Creator and annihilation operators operate in the usual manner

$$a|n\rangle = \sqrt{n}|n-1\rangle, \quad a^\dagger|n\rangle = \sqrt{n+1}|n+1\rangle \quad (1.20)$$

and $|0\rangle$ is the ground state such that $a|0\rangle = 0$. Energetic levels $E_n = \hbar\omega_c (n + \frac{1}{2})$ are quantized and degenerated. They are called *Landau levels*.

To eliminate the degeneration we need to define the guiding center coordinate (center of cyclotron motion) $\boldsymbol{\chi}$, that represent the barycentric coordinate²

$$\chi_x := x + \frac{1}{q_e B} \pi_y, \quad \chi_y := y - \frac{1}{q_e B} \pi_x \quad (1.21)$$

that satisfies

$$[\chi_x, \chi_y] = -il_B^2 \quad (1.22)$$

We observe, since the operators of guiding center components do not commute, the particle position cannot be determined more accurately than the area $2\pi l_B^2$. Furthermore

$$[\chi_x, \pi_x] = [\chi_x, \pi_y] = [\chi_y, \pi_x] = [\chi_y, \pi_y] = 0 \quad (1.23)$$

so the guiding center $\boldsymbol{\chi}$ and the covariant momentum $\boldsymbol{\pi}$ are entirely independent variables. We can construct one creation and one annihilation operator for which $[b, b^\dagger] = 1$,

$$b := \frac{1}{\sqrt{2}l_B} (\chi_x - i\chi_y), \quad b^\dagger := \frac{1}{\sqrt{2}l_B} (\chi_x + i\chi_y) \quad (1.24)$$

We observe that

$$[a, b] = [a^\dagger, b] = 1 \quad (1.25)$$

¹to obtain \mathbf{v} in quantum mechanics we use Heisenberg pictures. $\frac{d}{dt} r_i = \frac{i}{\hbar} [H, r_i]$

²in Heisenberg pictures, $\frac{d}{dt} \chi_i = 0$

so we have another independent harmonic oscillator $b^\dagger b |m\rangle = m |m\rangle$. The eigenstates of H_{EM} are the same of the number operator $M = b^\dagger b$, then the general eigenstate of the hamiltonian, with energy $E_n = \hbar\omega_c (n + \frac{1}{2})$ is a linear superposition of Fock states, which we call the *Landau sites*

$$|n, m\rangle = \sqrt{\frac{1}{n!m!}} (a^\dagger)^n (b^\dagger)^m |0, 0\rangle \quad (1.26)$$

where $|0, 0\rangle$ is the Fock vacuum. Their orthonormal completeness condition reads

$$\langle n_1, m_1 | n_2, m_2 \rangle = \delta_{n_1, n_2} \delta_{m_1, m_2}, \quad \sum_{n, m} |n, m\rangle \langle n, m| = 1 \quad (1.27)$$

The motion of an electron within one Landau level is specified by the guiding center χ . Since the coordinates χ_x and χ_y do not commute, we cannot diagonalize both of them simultaneously. It is necessary one of them or an appropriate combination of them to diagonalize.

1.3.1 Symmetric Gauge

We want to obtain the wave functions for the symmetric gauge:

$$\mathbf{A}(\mathbf{r}) = \left(-\frac{1}{2}By, \frac{1}{2}Bx, 0 \right) \quad (1.28)$$

Since the system has a disk geometry, it is appropriate to diagonalize the symmetric combination $\chi_x^2 + \chi_y^2$. It is equivalent to diagonalize the number operator $b^\dagger b$:

$$\chi_x^2 + \chi_y^2 = (2b^\dagger b + 1)l_B^2 \quad (1.29)$$

The Landau site $|n, m\rangle$ is an eigenstate of the operator $\chi_x^2 + \chi_y^2$

$$(\chi_x^2 + \chi_y^2) |n, m\rangle = (2m + 1)l_B^2 |n, m\rangle \quad (1.30)$$

The angular momentum operator is given by

$$L := xp_y - yp_x = (b^\dagger b - a^\dagger a)\hbar \quad (1.31)$$

so the state $|n, m\rangle$ has the angular momentum $(m - n)\hbar$ in a given Landau level n . b and b^\dagger are the operators increasing or decreasing the angular momentum.

Using a complex number $z := \frac{1}{l_B}(x + iy)$ for electron position³, the general solution for the states in the *lowest Landau level* (LLL), i.e. states which satisfy $a|0, m\rangle = 0$, is

$$\psi_{0, m}(\mathbf{r}) = h(z) \exp[-|z|^2/4] \quad (1.32)$$

where $h(z)$ is an arbitrary analytic function. All these states are degenerate.

The state $|0, 0\rangle$ satisfies $b|0, 0\rangle = 0$, which is solved as

$$\psi_{0, 0}(\mathbf{r}) = \frac{1}{\sqrt{2\pi l_B^2}} \exp\left(-\frac{r^2}{4l_B^2}\right) \quad (1.33)$$

The state $|0, m\rangle$ is described by the wave function

$$\psi_{0, m}(\mathbf{r}) = \sqrt{\frac{2^m}{2\pi l_B^2 m!}} z^m e^{-|z|^2/4} \quad (1.34)$$

It represent an electron circularly localized. The probability of finding the electron at $r = 2l_B|z|$ in the lowest Landau level is given by

$$|\psi_{0, m}(r)|^2 \propto r^{2m} \exp\left(-\frac{r^2}{2l_B^2}\right) \quad (1.35)$$

³We represent all the differential operators $a^\dagger, a, b^\dagger, b$ in term of z

which as a sharp peak at $r_m = \sqrt{2ml_B}$. These states are represented by rings on a disc geometry, where a ring is labeled by the angular momentum $m\hbar$. The area of each ring is

$$\Delta S = \pi r_{m+1}^2 - \pi r_m^2 = 2\pi l_B^2 \quad (1.36)$$

as is the area of one Landau site. The position of the electron cannot be localized within an area smaller than ΔS .

1.3.2 Landau Gauge

Now we consider the Landau Gauge, that is a good method to analyze the QH system with rectangular geometry. We suppose to have translational invariance in y direction.

$$\mathbf{A}(\mathbf{r}) = (0, Bx, 0) \quad (1.37)$$

Since we have $p_y = (\hbar/l_B^2)\chi_x$ conservation, we can diagonalize χ_x :

$$p_y |k_y\rangle = \hbar k_y |k_y\rangle, \quad \chi_x |k_y\rangle = k_y l_B^2 |k_y\rangle \quad (1.38)$$

Here k_y is a wave number in y direction.

To obtain the lowest Landau level, we have to apply LLL condition $a |k_y\rangle = 0$. Solving that differential equation is a trivial problem so:

$$\phi_{0,k_y}(\mathbf{r}) = \frac{1}{\pi^{1/4} l_B^{1/2}} \exp(ik_y y) \exp\left[-\frac{1}{2l_B^2}(x - k_y l_B^2)^2\right] \quad (1.39)$$

This is a plane wave propagating in y direction with momentum $\hbar k_y$. The probability finding electron at x has a sharp peak at $x = k_y l_B^2$. These states are represented by strips on a rectangular geometry, where a strip is labeled by the wave number k_y , located at $x = k_y l_B^2$, and has width $\delta x = l_B^2 \delta k_y$. Here $\delta k_y = 2\pi/L_y$, because the wave number is quantized as $k_y = 2\pi/L_y s_y$, where s_y is an integer and L_y is the y size of the system. The area of each strip is equal to

$$\Delta S = L_x \Delta y = 2\pi l_B^2 \quad (1.40)$$

as is the area of one Landau site.

1.3.3 Flux quanta and filling factor

Due to the Pauli exclusion principle only one electron can occupy one Landau site (spinless theory). Each of them has the area $\Delta S = 2\pi l_B^2$ so in each energy level the density of state ρ_Φ is

$$\rho_\Phi = \frac{N_\Phi}{S} = \frac{1}{2\pi l_B^2} \quad (1.41)$$

where S is the area of the total system and N_Φ is the number of states $S/\Delta S$. If we define the Dirac flux quantum Φ_D as the magnetic flux on the area ΔS ,

$$\Phi_D := 2\pi l_B^2 B = \frac{2\pi\hbar}{q_e} \quad (1.42)$$

the density of states is equal to the density of flux quanta

$$\rho_\Phi = \frac{N_\Phi}{S} = \frac{\Phi_{TOT}}{S\Phi_D} = \frac{B}{\Phi_D} \quad (1.43)$$

The filling fraction of the energy level is defined by the ratio

$$\nu = \frac{\text{Number of particles}}{\text{Number of states}} = \frac{S\rho_0}{S\rho_\Phi} = 2\pi l_B^2 \rho_0 = \frac{2\pi\hbar\rho_0}{q_e B} = \frac{\rho_0 \Phi_D}{B} \quad (1.44)$$

At $\nu = 1/q$ there are q flux quanta per electron, $B/\rho_0 = q\Phi_D$. The filling factor is called the *Landau level filling factor*, or simply the filling factor. When $\nu = 1$ the Landau level is full.

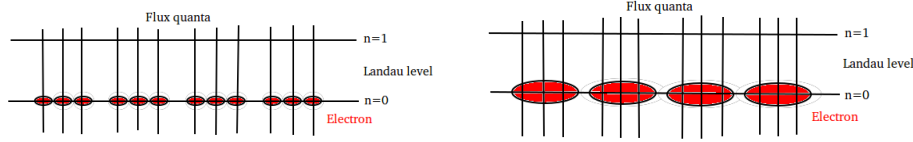


Figure 1.5: At $\nu = 1/q$ there are q flux quanta (vertical lines) per electron (circles). A composite particle (fermion or boson) is an electron bound to $(q - 1$ or $q)$ flux quanta. It behaves as a fat electron in the fractional QH state. Here we have $\nu = 1$ (left) and $\nu = 1/3$ (right).

1.4 Integer Quantum Hall effect

We have understood the quantum mechanical behavior of a particle in an electromagnetic field. We now consider a two-dimensional system of electrons in electromagnetic field. To avoid unnecessary complications we ignore the dynamical degree of freedom associated with spin by assuming that all spins are polarized and frozen by the Zeeman effect: it is a spin frozen system. We have an hamiltonian

$$H = \sum_i H_{EM}(\mathbf{r}_i, \mathbf{p}_i) + H_C \quad (1.45)$$

where $H_{EM}(\mathbf{r}_i, \mathbf{p}_i)$ is the electromagnetic hamiltonian for the i -th electron and H_C is the Coulomb energy contribution. Our first attempt to simplify the problem is neglecting the Coulomb energy, i.e. we use independent single-particle approximation. So we consider an hamiltonian

$$H = \sum_i H_{EM}(\mathbf{r}_i, \mathbf{p}_i) \quad (1.46)$$

Each electron can occupy only one Landau site, and the total eigenstate is a Slater determinant of single particle eigenstates. Working with this idealized system it can be demonstrated that we obtain classical prediction about Hall resistivity, because $\langle \mathbf{v}_i \rangle$ (mean i -th electron's speed value calculated on Landau sites) has the same behavior of the classical speed.

To understand IQHE it is necessary to introduce the interaction of the system with impurities, defects and inhomogeneity [13]. This theory was provided by Laughlin in 1981 [14]. We need strong magnetic fields so that Landau levels don't intersect. Essentially the interaction with impurities partially splits Landau sites and broadens Landau levels. However new single-particle states of the system aren't equivalent. States in the tail of new Landau levels are Anderson localized, thus they are ensnared in a specific microscopic region of the system. So disorder traps electrons wave functions. At the opposite, states near the center of new Landau levels aren't localized, they are extended on all the system.

Only extended wave functions can contribute to current flow. Let us analyze the behaviour of a low temperature system varying the particle density. For low densities, all particles occupy localized states and current flow is impossible. Adding particles, Fermi energy reaches first possible Landau level, a region with extended states, and conductivity gains one quantum e^2/h . Next density level cross the other tail of Landau level that is a region with localized states. So conductivity remains constant and has a plateau. Increasing density means refreshing the sequence. At each Landau level conductivity has a leap. Laughlin connects changes in magnetic field to density mutations through flux quanta filling fraction [15].

1.5 Fractional Quantum Hall effect

The FQHE is most pronounced when the magnetic field is so strong that the lowest Landau level is partially filled on. In this case, the ground state of noninteracting electrons is highly degenerate, a prerequisite for the appearance of fractional charges. But instead of a noninteracting system, we are dealing here with a strongly correlated system [16]. The kinetic energy of the electrons is practically reduced to zero where the zero point fluctuations $\hbar\omega_c/2$ of the cyclotron frequency remain. Therefore the Coulomb repulsion of the electrons dominates and the ground state must

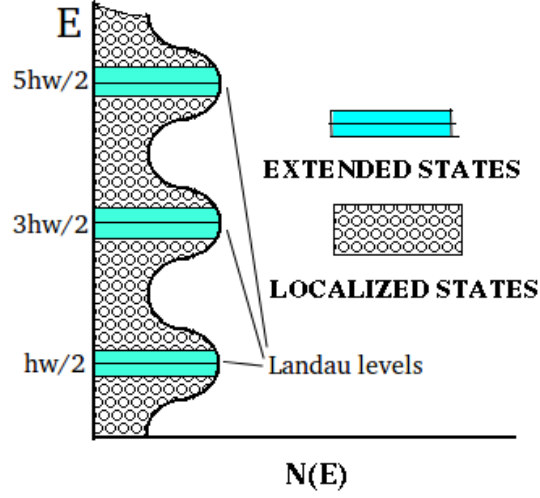


Figure 1.6: Extended and localized states. We can explain IQHE supposing that impurities and defects broaden Landau levels. States in the tail of new Landau levels are Anderson localized, states near the center of new Landau levels are extended.

minimize it. In order to minimize the Coulomb repulsion of the electrons we have to find a proper superposition of Slater determinants. Because the general eigenfunction for single particle LLL is

$$\psi_{0,m}(\mathbf{r}) = h(z) \exp[-|z|^2/4] \quad (1.47)$$

we assume that superposition for LLL is of the general form

$$\psi(\mathbf{r}_1, \dots, \mathbf{r}_N) = h(z_1, \dots, z_N) \exp\left[-\sum_i |z_i|^2/4\right] \quad (1.48)$$

Using symmetry assumptions (angular momentum conservation and Pauli's principle) Laughlin proposed his ansatz [\[4\]](#)

$$\psi(\mathbf{r}_1, \dots, \mathbf{r}_N) = \prod_{i < j} (z_i - z_j)^m \exp\left[-\sum_i |z_i|^2/4\right], \quad m = 1, 3, 5, \dots \quad (1.49)$$

Next we have to find the proper value of m for a given filling factor of the lowest Landau level, or the right filling factor ν for a given value of m . Refer to specific texts for discussion.

Chapter 2

TT hamiltonian

Theories until now exposed that attempt to explain the Fractional Quantum Hall effect (FQHE) have a phenomenological approach. In 1983 R. Tao and D. J. Thouless (TT) proposed a microscopic approach to FQHE [1]. They suggested that electrons in a strong magnetic field could form a one dimensional *Wigner crystal* [2] in the lattice *target space* of the lowest Landau Level (LLL). This weird electron crystal was responsible, in their opinion, of the observed fractional quantization of the Hall resistivity. They motivated their claim with an Hartree-Fock analysis of the complete second quantization Hamiltonian for N interacting electrons in a magnetic field restricted to the LLL.

However their microscopic theory was later abandoned (by Thouless in first person [3]) because it was in conflict with the celebrated phenomenological *Laughlin's ansatz* [4] for the wave function of the $\nu = 1/q$ odd filling factors Quantum Hall states. In a nutshell, TT wave function has long-range spatial correlations (due to the Wigner crystal formation) that Laughlin wavefunction does not display. There are two strong points in favor of Laughlin's theory. The first is that the overlap of LW with the exact ground state for a small number of electrons is extremely large. The second is that the odd denominators for fractional quantization follow very naturally from Laughlin's theory.

Taking a cue from some recent works that analyze the theory of TT in some special physical limits [17], here we argue that TT theory foundations were not completely wrong, by exhibiting an exact analysis of the Quantum Hall Hamiltonian in the LLL. Our analysis suggests that Wigner crystals play a fundamental role in Quantum Hall physics. However, as we explicitly show, Wigner crystals form in the *momentum* target space of the LLL, thus eliminating long range spatial correlations of the macroscopic wavefunction. Using results of the next chapter, as a byproduct of our analysis we argue that FQHE is nothing but a pathological phase transition, typical of lattice gases with repulsive long range interactions [18].

2.1 Microscopic model

We consider a standard two-dimensional electron gas model, with interacting electrons moving in a uniform positive background to form an electrically neutral system. We also assume that the magnetic field is so strong that the Coulomb interaction does not significantly mix different Landau levels, thus we work in the regime: $q_e^2/l \ll \omega_c$, with $l = 1/(q_e B)^{1/2}$ being the magnetic length and $\omega_c = q_e B/m_e$ the cyclotron frequency ($\hbar = c = 1$). For simplicity we assume that all electrons are in the lowest spin polarized, so $\nu < 1$, but there is no difficulty in generalizing the discussion to higher Landau levels.

We take the system to have area L^2 and rectangular geometry, so that the single particle wave functions in LLL may be written in the form

$$\langle \mathbf{r} | 0, k_y \rangle = \phi_{0, k_y}(\mathbf{r}) = \frac{1}{\pi^{1/4} (lL)^{1/2}} \exp(ik_y y) \exp \left[-\frac{1}{2l^2} (x - k_y l^2)^2 \right] \quad (2.1)$$

We take the system to be periodic in the y direction, so periodic boundary conditions are assumed

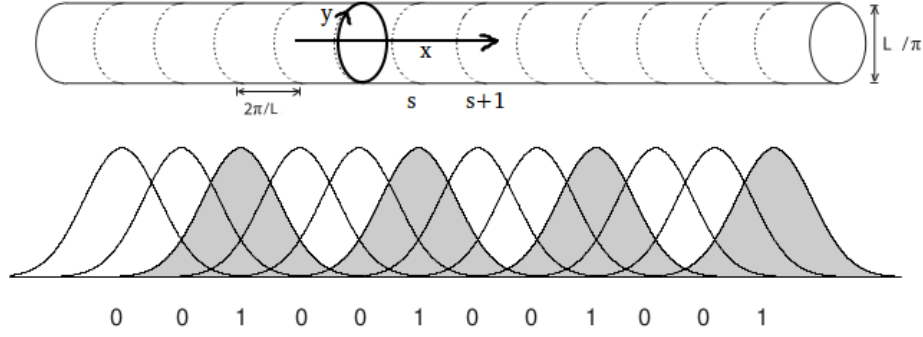


Figure 2.1: Lowest Landau sites in our model are represented by strips in cylindrical geometry and each strip is labeled by the quantum wave number s . Image taken from [17].

and k_y can take the values

$$k_y = \frac{2\pi}{L}s \quad (2.2)$$

where s is an integer. The allowed values of s are further restricted by the condition that the center of force of the oscillator, $x_0 := k_y l^2$, must physically lie within the system, $0 \leq x_0 < L$. This gives the following range for s ,

$$0 \leq s < N_s, \quad N_s := \frac{L^2}{2\pi l^2} \quad (2.3)$$

Then the single particle wave functions in LLL may be written in the form

$$\langle \mathbf{r} | 0, s \rangle = \phi_{0,s}(x, y) = \frac{1}{\pi^{1/4}(lL)^{1/2}} \exp\left[\frac{2\pi i s y}{L}\right] \exp\left[-\frac{1}{2}\left(\frac{x}{l} - \frac{2\pi s l}{L}\right)^2\right] \quad (2.4)$$

Since we want solve the exact microscopic model, we assume to have an hamiltonian in first quantization

$$H = \sum_i H_{EM}(i) + \sum_{i>j} H_C(i, j) \quad (2.5)$$

where $H_{EM}(i)$ is the electromagnetic hamiltonian for the i -th electron and $H_C(i, j)$ is the Coulomb energy contribution, that we don't neglect. We can rewrite this in second quantization, using Fock-space operators, on LLL bases $|0, s\rangle := |s\rangle$

$$H = \sum_{s_1, s_2=0}^{N_s-1} \langle s_1 | H_{EM} | s_2 \rangle a_{s_1}^\dagger a_{s_2} + \frac{1}{2} \sum_{s_1, s_2, s_3, s_4=0}^{N_s-1} \langle s_1, s_2 | H_C | s_3, s_4 \rangle a_{s_1}^\dagger a_{s_2}^\dagger a_{s_3} a_{s_4} \quad (2.6)$$

where a_s^\dagger, a_s are fermionic creation and annihilation operators of a particle in $|s\rangle$ state. We are able to calculate the first contribution

$$\sum_{s_1, s_2=0}^{N_s-1} \langle s_1 | H_{EM} | s_2 \rangle a_{s_1}^\dagger a_{s_2} = \sum_{s_1, s_2=0}^{N_s-1} \langle s_1 | \omega_c \left(a^\dagger a + \frac{1}{2}\right) | s_2 \rangle a_{s_1}^\dagger a_{s_2} \quad (2.7)$$

$$= \frac{1}{2} \omega_c \sum_{s_1, s_2=0}^{N_s-1} \delta_{s_1, s_2} a_{s_1}^\dagger a_{s_2} \quad (2.8)$$

$$= \frac{1}{2} \omega_c \sum_{s=0}^{N_s-1} a_s^\dagger a_s = \frac{1}{2} \omega_c \sum_{s=0}^{N_s-1} n_s \quad (2.9)$$

where n_s is number operator. The Coulomb term can be written in the form [\[1\]](#)

$$\frac{1}{2} \sum_{s_1, s_2, s_3, s_4=0}^{N_s-1} \langle s_1, s_2 | H_C | s_3, s_4 \rangle a_{s_1}^\dagger a_{s_2}^\dagger a_{s_3} a_{s_4} = \frac{1}{2} \sum_{s_1, s_2, s_3, s_4=0}^{N_s-1} V(s_1 - s_3, s_2 - s_3) a_{s_1}^\dagger a_{s_2}^\dagger a_{s_3} a_{s_4} \delta_{s_1+s_2, s_3+s_4} \quad (2.10)$$

where the Coulomb matrix element is given by

$$V(s_1 - s_3, s_2 - s_3) = \frac{e^2}{L} \int_{-\infty}^{\infty} dq \frac{\exp \left[-\frac{l^2}{2} \left(q^2 + \frac{4\pi^2 (s_1 - s_3)^2}{L^2} \right) + \frac{2\pi i q l^2 (s_2 - s_3)}{L} \right]}{\sqrt{q^2 + \frac{4\pi^2 (s_1 - s_3)^2}{L^2}}}. \quad (2.11)$$

2.2 TT Coulomb matrix element

We want to evaluate the integral [\(2.11\)](#) in the physical limit $L/l \gg 1$, i.e. when system's dimension is bigger than magnetic length. This is a good physical approximation because $B = 10 T$ means $l \simeq 10 nm$. We start writing the integral in term of N_s

$$V(s_1 - s_3, s_2 - s_3) = \frac{e^2}{L} \int_{-\infty}^{\infty} dq \frac{\exp \left[-\frac{l^2}{2} \left(q^2 + \frac{2\pi N_s (s_1 - s_3)^2}{l^2 N_s^2} \right) + iL \frac{(s_2 - s_3)}{N_s} q \right]}{\sqrt{q^2 + \frac{2\pi N_s (s_1 - s_3)^2}{l^2 N_s^2}}}. \quad (2.12)$$

then, using the substitution $q = (L/l^2)t$

$$V(s_1 - s_3, s_2 - s_3) = \frac{e^2}{L} \int_{-\infty}^{\infty} dt \frac{\exp \left[\frac{L^2}{l^2} \left(-\frac{t^2}{2} - \frac{(s_1 - s_3)^2}{2N_s^2} + i \frac{(s_2 - s_3)}{N_s} t \right) \right]}{\sqrt{t^2 + \frac{(s_1 - s_3)^2}{N_s^2}}}. \quad (2.13)$$

and using Euler's formula $e^{ix} = \cos(x) + i \sin(x)$,

$$V(s_1 - s_3, s_2 - s_3) = \frac{e^2}{L} \int_{-\infty}^{\infty} dt \frac{\cos \left[\frac{L^2}{l^2} \left(\frac{(s_2 - s_3)}{N_s} t \right) \right] \exp \left[\frac{L^2}{l^2} \left(-\frac{t^2}{2} - \frac{(s_1 - s_3)^2}{2N_s^2} \right) \right]}{\sqrt{t^2 + \frac{(s_1 - s_3)^2}{N_s^2}}} \quad (2.14)$$

$$+ i \frac{e^2}{L} \int_{-\infty}^{\infty} dt \frac{\sin \left[\frac{L^2}{l^2} \left(\frac{(s_2 - s_3)}{N_s} t \right) \right] \exp \left[\frac{L^2}{l^2} \left(-\frac{t^2}{2} - \frac{(s_1 - s_3)^2}{2N_s^2} \right) \right]}{\sqrt{t^2 + \frac{(s_1 - s_3)^2}{N_s^2}}} \quad (2.15)$$

Imaginary part of integral is null because it is an odd function on even domain. So the integral that we have to approximate becomes

$$V(s_1 - s_3, s_2 - s_3) = \frac{e^2}{L} \int_{-\infty}^{\infty} dt \frac{\cos \left[\frac{L^2}{l^2} \left(\frac{(s_2 - s_3)}{N_s} t \right) \right] \exp \left[\frac{L^2}{l^2} \left(-\frac{t^2}{2} - \frac{(s_1 - s_3)^2}{2N_s^2} \right) \right]}{\sqrt{t^2 + \frac{(s_1 - s_3)^2}{N_s^2}}} \quad (2.16)$$

This matrix element could be evaluated exactly in the physical limit $\lambda := L^2/l^2 \gg 1$ by the saddle point method, because we have only intensive function of t , i.e.

$$0 \leq s_i < N_s \quad \Rightarrow \quad 0 \leq \frac{|s_i - s_j|}{N_s} < 1 \quad (2.17)$$

If $\lambda \rightarrow \infty$ and $f(z)$ is regular in z_0 , then

$$I(\lambda) = \int_C dz f(z) e^{\lambda g(z)} \sim f(z_0) e^{\lambda g(z_0)} e^{i\theta} \left(\frac{2\pi}{\lambda a} \right)^{\frac{1}{2}} \quad (2.18)$$

where we define

- z_0 such that $g'(z_0) = 0$

- a such that $g''(z_0) = ae^{i\alpha}$
- θ such that $\theta = \frac{\pi - \alpha}{2}$

We are now ready to evaluate the integral. Defining, compatibly with the previous notation,

$$f(t) := \frac{e^2}{L} \frac{\cos \left[\frac{L^2}{l^2} \left(\frac{(s_2 - s_3)t}{N_s} \right) \right]}{\sqrt{t^2 + \frac{(s_1 - s_3)^2}{N_s^2}}}, \quad g(t) := -\frac{t^2}{2} - \frac{(s_1 - s_3)^2}{2N_s^2} \quad (2.19)$$

we obtain

$$V(s_1 - s_3, s_2 - s_3) \sim \frac{e^2}{L} \frac{N_s}{|s_1 - s_3|} \left(\frac{2\pi l^2}{L^2} \right)^{\frac{1}{2}} \exp \left[-2\pi \frac{(s_1 - s_3)^2}{N_s} \right] \quad (2.20)$$

$$= \frac{e^2}{(2\pi)^{1/2} l} \frac{1}{|s_1 - s_3|} \exp \left[-2\pi \frac{(s_1 - s_3)^2}{N_s} \right] \quad (2.21)$$

We observe that, in the physical limit $L/l \gg 1$, the integral (2.11) doesn't depend on the difference $(s_2 - s_3)$, it depend only on $|s_1 - s_3|$ so it is translationally invariant and it is a *screened Coulomb potential* (see Figure 2.2).

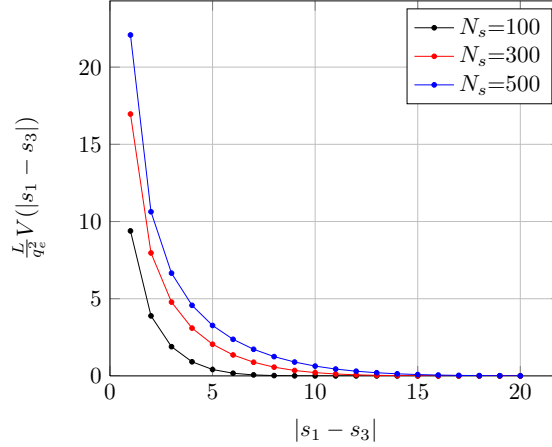


Figure 2.2: TT Coulomb matrix element (2.11) in the limit $L^2/l^2 \gg 1$. If we take $L \sim 1\mu\text{m}$ then $N_s = 100, N_s = 300, N_s = 500$ correspond respectively to $B = 2.5T, B = 7.5T, B = 13T$.

2.3 Momentum target space

We have obtained that, in the physical limit $L/l \gg 1$, the hamiltonian can be written

$$H = \frac{1}{2} \omega_c \sum_{s=0}^{N_s-1} n_s + \frac{1}{2} \sum_{s_1, s_2, s_3, s_4=0}^{N_s-1} V(|s_1 - s_3|) a_{s_1}^\dagger a_{s_2}^\dagger a_{s_4} a_{s_3} \delta_{s_1+s_2, s_3+s_4} \quad (2.22)$$

Thus electrons in the LLL form a one dimensional lattice (that in the following we will call *target space*) and they interact through a long range translational invariant (in the target space) interaction. This suggests that the Hamiltonian may be readily diagonalized in momentum target space, by the definition of the new operators:

$$c_k^\dagger := \frac{1}{\sqrt{N_s}} \sum_{s=0}^{N_s-1} e^{-\frac{2\pi i}{N_s} sk} a_s^\dagger, \quad c_k := \frac{1}{\sqrt{N_s}} \sum_{s=0}^{N_s-1} e^{\frac{2\pi i}{N_s} sk} a_s \quad (2.23)$$

They are the discrete Fourier transform (DFT) of a_s^\dagger, a_s . Inverse transformation is:

$$a_s^\dagger = \frac{1}{\sqrt{N_s}} \sum_{k=0}^{N_s-1} e^{\frac{2\pi i}{N_s} s k} c_k^\dagger, \quad a_s = \frac{1}{\sqrt{N_s}} \sum_{k=0}^{N_s-1} e^{-\frac{2\pi i}{N_s} s k} c_k \quad (2.24)$$

Remembering that

$$\sum_{s=0}^{N_s-1} e^{-\frac{2\pi i}{N_s} s k} = N_s \delta_{k,0} \quad (2.25)$$

the electromagnetic hamiltonian becomes

$$\sum_{s=0}^{N_s-1} n_s = \frac{1}{N_s} \sum_{s=0}^{N_s-1} \sum_{k_1, k_2=0}^{N_s-1} e^{\frac{2\pi i}{N_s} s(k_1-k_2)} c_{k_1}^\dagger c_{k_2} \quad (2.26)$$

$$= \sum_{k_1, k_2=0}^{N_s-1} c_{k_1}^\dagger c_{k_2} \delta_{k_1, k_2} \quad (2.27)$$

$$= \sum_{k=0}^{N_s-1} n_k \quad (2.28)$$

Now we have to transform the Coulomb matrix element. First we solve the delta function $\delta_{s_1+s_2, s_3+s_4}$, remembering that $0 \leq s_4 < N_s$:

$$\sum_{s_1, s_2, s_3, s_4=0}^{N_s-1} V(|s_1 - s_3|) a_{s_1}^\dagger a_{s_2}^\dagger a_{s_4} a_{s_3} \delta_{s_1+s_2, s_3+s_4} \quad (2.29)$$

$$= \sum_{s_1, s_2, s_3=0}^{N_s-1} V(|s_1 - s_3|) a_{s_1}^\dagger a_{s_2}^\dagger a_{s_1+s_2-s_3} a_{s_3} \theta_{s_1+s_2-s_3} \theta_{N_s-s_1-s_2+s_3-1} \quad (2.30)$$

then, using the DFT,

$$= \frac{1}{(N_s)^2} \sum_{s_1, s_2, s_3=0}^{N_s-1} \sum_{k_1, k_2, k_3, k_4=0}^{N_s-1} V(|s_1 - s_3|) e^{\frac{2\pi i}{N_s} [s_1(k_1-k_3)+s_2(k_2-k_3)+s_3(k_3-k_4)]} c_{k_1}^\dagger c_{k_2}^\dagger c_{k_3} c_{k_4} \times \quad (2.31)$$

$$\times \theta_{s_1+s_2-s_3} \theta_{N_s-s_1-s_2+s_3-1} \quad (2.32)$$

$$= \frac{1}{(N_s)^2} \sum_{k_1, k_2, k_3, k_4=0}^{N_s-1} c_{k_1}^\dagger c_{k_2}^\dagger c_{k_3} c_{k_4} \sum_{s_1, s_2, s_3=0}^{N_s-1} V(|s_1 - s_3|) e^{\frac{2\pi i}{N_s} [s_1(k_1-k_3)+s_2(k_2-k_3)+s_3(k_3-k_4)]} \quad (2.33)$$

$$\times \theta_{s_1+s_2-s_3} \theta_{N_s-s_1-s_2+s_3-1} \quad (2.34)$$

introducing the variable $s = s_1 - s_3$, remembering that $0 \leq s_3 < N_s$ and $-N_s < s < N_s$,

$$= \frac{1}{(N_s)^2} \sum_{k_1, k_2, k_3, k_4=0}^{N_s-1} c_{k_1}^\dagger c_{k_2}^\dagger c_{k_3} c_{k_4} \sum_{s_1, s_2=0}^{N_s-1} \sum_{s=1-N_s}^{N_s-1} V(|s|) e^{\frac{2\pi i}{N_s} [s_1(k_1-k_4)+s_2(k_2-k_3)-s(k_3-k_4)]} \times \quad (2.35)$$

$$\times \theta_{s+s_2} \theta_{N_s-s-s_2-1} \theta_{s_1-s} \theta_{N_s-s_1+s-1} \quad (2.36)$$

Now we can break the s sum in three parts, solving theta functions,

$$= \frac{1}{(N_s)^2} \sum_{k_1, k_2, k_3, k_4=0}^{N_s-1} c_{k_1}^\dagger c_{k_2}^\dagger c_{k_3} c_{k_4} \sum_{s_1, s_2=0}^{N_s-1} \sum_{s=1}^{N_s-1} V(|s|) e^{\frac{2\pi i}{N_s} [s_1(k_1-k_4)+s_2(k_2-k_3)-s(k_3-k_4)]} \theta_{N_s-s-s_2-1} \theta_{s_1-s} \quad (2.37)$$

$$+ \frac{1}{(N_s)^2} \sum_{k_1, k_2, k_3, k_4=0}^{N_s-1} c_{k_1}^\dagger c_{k_2}^\dagger c_{k_3} c_{k_4} \sum_{s_1, s_2=0}^{N_s-1} \sum_{s=1-N_s}^{-1} V(|s|) e^{\frac{2\pi i}{N_s} [s_1(k_1-k_4)+s_2(k_2-k_3)-s(k_3-k_4)]} \theta_{s+s_2} \theta_{N_s-s_1+s-1} \quad (2.38)$$

$$+ \frac{1}{(N_s)^2} \sum_{k_1, k_2, k_3, k_4=0}^{N_s-1} c_{k_1}^\dagger c_{k_2}^\dagger c_{k_3} c_{k_4} \sum_{s_1, s_2=0}^{N_s-1} V(0) e^{\frac{2\pi i}{N_s} [s_1(k_1-k_4)+s_2(k_2-k_3)]} \quad (2.39)$$

$$= \frac{1}{(N_s)^2} \sum_{k_1, k_2, k_3, k_4=0}^{N_s-1} c_{k_1}^\dagger c_{k_2}^\dagger c_{k_3} c_{k_4} \sum_{s_1, s_2=0}^{N_s-1} \sum_{s=1}^{N_s-1} V(s) e^{\frac{2\pi i}{N_s} [s_1(k_1-k_4) + s_2(k_2-k_3) - s(k_3-k_4)]} \theta_{N_s-s-s_2-1} \theta_{s_1-s} \quad (2.40)$$

$$+ \frac{1}{(N_s)^2} \sum_{k_1, k_2, k_3, k_4=0}^{N_s-1} c_{k_1}^\dagger c_{k_2}^\dagger c_{k_3} c_{k_4} \sum_{s_1, s_2=0}^{N_s-1} \sum_{s=1}^{N_s-1} V(s) e^{\frac{2\pi i}{N_s} [s_1(k_1-k_4) + s_2(k_2-k_3) + s(k_3-k_4)]} \theta_{s_2-s} \theta_{N_s-s_1-s-1} \quad (2.41)$$

$$+ \sum_{k_1, k_2=0}^{N_s-1} V(0) n_{k_1} n_{k_2} \quad (2.42)$$

So, we conclude this sections observing that, in the physical limit $L/l \gg 1$, the hamiltonian (2.11) in momentum space is diagonal and it can be written

$$H = \frac{1}{2} \omega_c \sum_{k=0}^{N_s-1} n_k + \frac{1}{2} \sum_{k_1, k_2=0}^{N_s-1} \tilde{V}(|k_1 - k_2|) n_{k_1} n_{k_2} \quad (2.43)$$

with (see Figure 2.3)

$$\tilde{V}(|k_1 - k_2|) = \sum_{s=0}^{N_s-1} V(s) \exp \left[\frac{2\pi i}{N_s} s(k_1 - k_2) \right] \quad (2.44)$$

There is a deep physical meaning in this hamiltonian. We observe that our model in momentum space seems something like a one dimensional lattice gas: indeed we have an hamiltonian that depends only on occupation numbers n_k where k_i is i -th site's index. So an occupied site it is like a momentum-particle. Only occupied sites interact. Our model is long range because not only nearest neighbor sites interact. We observe that the number of effective physical electrons N_0 in LLL (i.e. the number of occupied sites in direct space) and the number of momenta-particles (i.e. the number of occupied sites in momentum space) are equal because of (2.28). From that we obtain a conservation law for the filling factor $\nu = N_0/N_s$ under Fourier transform of the hamiltonian. This is a key element because we think that filling factors are microscopic observable quantities related to macroscopic Hall resistivity (or conductivity).

2.4 Mapping on long-range repulsive lattice gas

(2.43) represents an hamiltonian of one-dimensional long-range repulsive lattice gas in canonical ensemble. If we use the grandcanonical ensemble, i.e. we fix the number of states N_s but we can change the number of momentum-particles N_0 , we can add to the hamiltonian a Lagrange multiplier, the chemical potential μ , so, in momentum space:

$$H = -\mu \sum_{k=0}^{N_s-1} n_k + \frac{1}{2} \sum_{k_1, k_2=0}^{N_s-1} \tilde{V}(|k_1 - k_2|) n_{k_1} n_{k_2} \quad (2.45)$$

We depth study this hamiltonian, that we call *Hubbard's hamiltonian in grandcanonical ensemble* or *Bak's hamiltonian* in third chapter 18.

In next chapter we suppose that $\tilde{V}(k)$ belongs to a class of potentials, those satisfying the two conditions:

$$V(k) \rightarrow 0 \quad \text{as } k \rightarrow \infty \quad (2.46)$$

$$V(k+1) + V(k-1) \geq 2V(k) \quad \text{for all } k > 1 \quad (2.47)$$

Second conditions means that potential must be strictly convex. In our specific hamiltonian (2.45), where the potential behaves as in Figure 2.3 we see numerically that:

- $\tilde{V}(k) \rightarrow -K_1(N_s)$ as $k \rightarrow N_s/2$, i.e $\tilde{V}(k)$ tends to a negative constant that depends on N_s and not to 0;

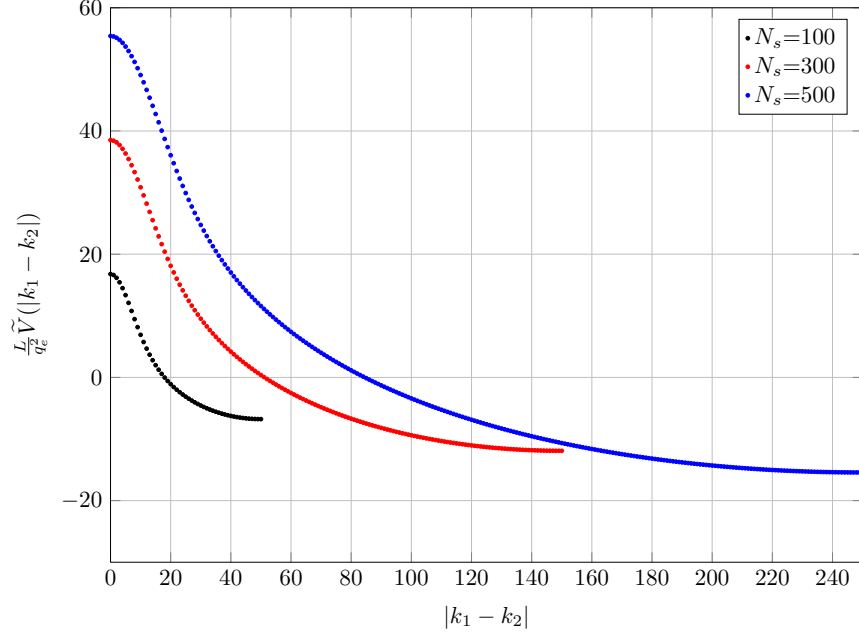


Figure 2.3: TT Coulomb matrix element (2.11) in the limit $L^2/l^2 \gg 1$ in momentum space. If we take $L \sim 1\mu\text{m}$ then $N_s = 100, N_s = 300, N_s = 500$ correspond respectively to $B = 2.5T, B = 7.5T, B = 13T$. We observe that (2.11) is concave near $|k_1 - k_2| = 0$ and the concavity depends on N_s . Moreover \tilde{V} tends to a negative constant that depends on N_s .

- $\tilde{V}(k)$ is concave near the $k = 0$ point and the concavity depends on N_s , i.e. $\tilde{V}(k+1) + \tilde{V}(k-1) \leq 2\tilde{V}(k)$ for $0 < k < K_2(N_s)$.

So we are not studying exactly the same problem that we encounter in third chapter. Only to understand the physics of the calculated potential, we ignore this differences for a moment: we would like to use analytical results of the next chapter. Observing the behavior of (2.44) at big distances, we consider $\tilde{V}(k)$ as a Coulomb potential (we cut the concave part),

$$\tilde{V}(|k_1 - k_2|) \sim \frac{e^2}{\sqrt{2\pi}l} \frac{1}{|k_1 - k_2|} \quad (2.48)$$

where the factor $1/l \sim B^{1/2}$ (that we see in non-approximated potential (2.44)) represents a scaling factor, that change the physics of the model. Indeed, if we consider the hamiltonian H' , that we will study exactly in third chapter and for which we know phase diagram:

$$H' := lH = -\mu l \sum_{k=0}^{N_s-1} n_k + \frac{e^2}{\sqrt{8\pi}} \sum_{k_1, k_2=0}^{N_s-1} \frac{1}{|k_1 - k_2|} n_{k_1} n_{k_2} \quad (2.49)$$

$$\sim -B^{-1/2} \sum_{k=0}^{N_s-1} n_k + \frac{e^2}{\sqrt{8\pi}} \sum_{k_1, k_2=0}^{N_s-1} \frac{1}{|k_1 - k_2|} n_{k_1} n_{k_2} \quad (2.50)$$

we see that we can compare $B^{-1/2}$ to Bak's chemical potential h . What does it means? B represent our external field that changes the system's state. Since we know the structure of Bak's hamiltonian, we are able to quantify how this field modifies the apparatus.

Physically the system will tend to occupy the state that minimize the hamiltonian (2.45). Changes in external field B could cause perturbations of the previous ground state, and then the system could change or not change its condition. So, the essential feature to analyze to understand

how the system reacts to B , it's a phase diagram, or a diagram that indicates which phase corresponds to specific B value. What is the key element that identifies only one phase? From Bak's model we learn that is the particles density ρ . So, in this case, it is the filling factor ν , that is the density of momentum particles (or electrons) on density of states.

We know the phase diagram for $h = B^{-1/2}$, i.e $\nu(h)$ (see chapter 3). We have only to change the independent variable h to plot the diagram in term of B . We can use the transformation $\nu(B) = \nu(h(B))$ so we have to associate the value $\nu(h)$ to the point $h^{-2} = B$. Results are in Figure 2.4

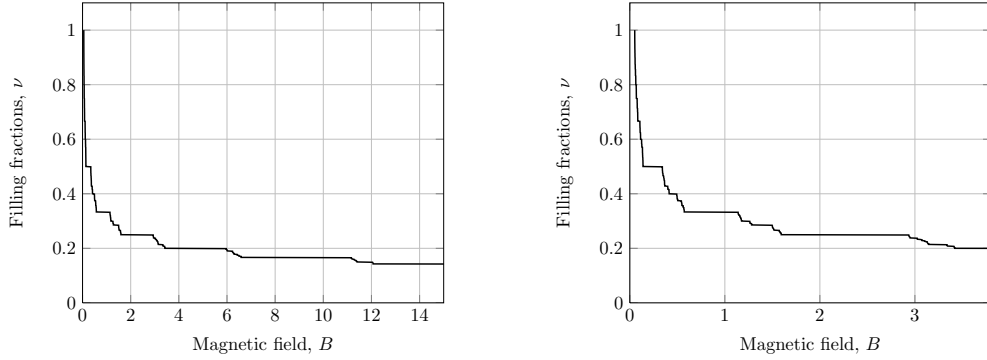


Figure 2.4: Phase diagram $\nu(B)$ (or stability diagram) for the hamiltonian (2.49) with Coulomb potential (2.48). It shows the *Devil's Staircase*. We observe that the scaling factor $1/l \sim B^{1/2}$ in potential expression represents the origin of different plateau length for fractions p/q and $1 - p/q$. Absolute B values have not physical meaning, they are only relative. We observe that increasing B means decreasing $\nu = N_0/N_s$, indeed we are increasing N_s , number of states, for constant N_0 , number of particles.

Phase diagram $\nu(B)$ has a plateau structure similar to the graphs of collected data on the Hall conductivity $\sigma_{xy}(B)$. It is a good indication that the search is taking its steps in the right direction. However there are important differences between the two physical quantities, which would require the full comprehension of the link between the filling fractions and conductivity in quantum mechanics to be evaluated. As it can be observed, in correspondence with the filling fractions with even denominator, the conductivity does not have a plateau but decreases linearly, in a "classic way".

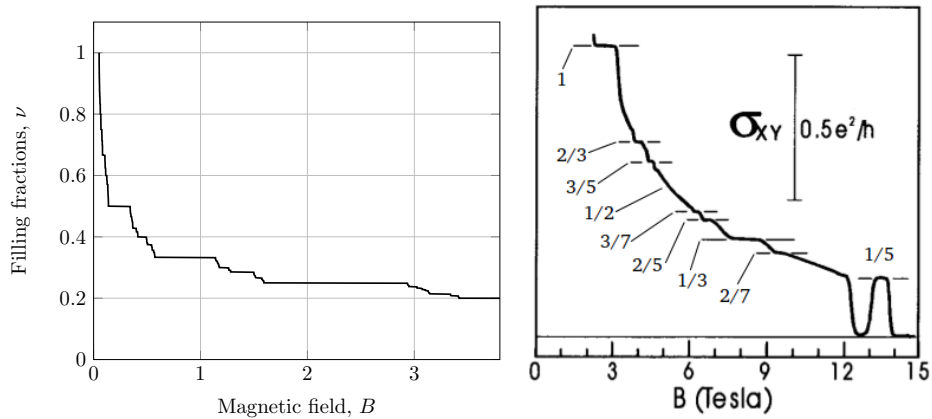


Figure 2.5: Calculated phase diagram $\nu(B)$ versus experimental data for Hall conductivity $\sigma_{xy}(B)$.

Chapter 3

Lattice gas models

3.1 Introduction

In this chapter we study one-dimensional lattice gas models, paying particular attention to how the range of interactions between discrete sites entirely changes the physics of the system. Starting from classical nearest-neighbor Ising models, of which you know the thermodynamics, we will analyze low temperature systems with long-range interactions, showing how the collective effects give rise to pathological phase transitions, that we will call *Devil's Staircase* [18].

The reader may profitably consult [19, 20, 21] to have an introduction on Ising models.

3.2 The Ising model

3.2.1 Definition of the model

In his 1924 thesis, Ernst Ising introduced a mathematical model that attempted to simulate the structure of a physical ferromagnetic substance, using tools from statistical mechanics. The scientific interest for this model comes from the fact that it can be used to solve a large class of problems, not necessarily related to magnetism in materials. What we call *Ising model* corresponds to a set of models that share the foundation: interacting $\frac{1}{2}$ -spins on a lattice.

In the Ising models the system considered is an array of N fixed points called lattice sites that form an d -dimensional periodic lattice Λ , which has a fixed spacial geometry. Associated with each lattice site $i \in \Lambda$ is a spin variable σ_i ($i = 1, \dots, N$) which is a number that is either $+1$ or -1 . There are no other variables. A given set of numbers $\boldsymbol{\sigma} = \{\sigma_i\}$ specifies a configuration (microstate) of the whole system. The whole lattice is then capable of 2^N configurations.

Associated with each configuration there is an energy E that arises from mutual interactions among the sites of the lattice (supposed to be two-body interaction) and from the interaction of the whole lattice with an external field h . In the Ising models it is

$$E(\boldsymbol{\sigma}) = - \sum_{i,j=1}^N J_{ij} \sigma_i \sigma_j - \sum_{i=1}^N h_i \sigma_i \quad (3.1)$$

where the minus sign on each term of the energy is conventional. From the theoretical point of view these hypotheses would be sufficient to obtain the thermodynamic of this model with the tools of statistical mechanics: we have microstates and their energy, we suppose that probabilities are Boltzmann weights, we can construct partition function:

$$Z = \sum_{\boldsymbol{\sigma}} e^{-\beta E(\boldsymbol{\sigma})} = \sum_{\sigma_1} \dots \sum_{\sigma_N} e^{-\beta E(\boldsymbol{\sigma})} \quad (3.2)$$

and than obtain thermodynamic functions in the usual manner from the Helmholtz free energy:

$$A = -k_B T \ln Z \quad (3.3)$$

However, the problem is too general for a solution. It is necessary to make further assumptions about the type of interaction to obtain analytical results.

3.2.2 Classification of models

Key elements that allow the classification of the models are the properties of exchange interactions J_{ij} .

First Ising models are classified according to the signs of spins interaction. If $J_{ij} > 0$, for all pairs $i, j \in \Lambda$, the interaction is called *ferromagnetic* and spins tend to be parallel. Conversely if $J_{ij} < 0$, for all pairs $i, j \in \Lambda$, the interaction is called *antiferromagnetic* and spins tend to be antiparallel. We can also have $J_{ij} = 0$ and spins are noninteracting. Otherwise the system is called *nonferromagnetic*.

Second we can distinguish Ising models according to the length of spins interaction. Typically, the exchange interaction falls off rapidly as the separation of the two spins is increased. We may regard it as negligible for all but nearest-neighbor pairs: these are *short-range models*. Assuming the symbol $\langle ij \rangle$ denotes a nearest-neighbor pair of spins, energy becomes

$$E(\boldsymbol{\sigma}) = - \sum_{\langle ij \rangle} J_{ij} \sigma_i \sigma_j - \sum_{i=1}^N h_i \sigma_i \quad (3.4)$$

The sum over $\langle ij \rangle$ contains $\gamma N/2$ terms, where γ is the number of nearest-neighbors of any given site (coordination number) and it depends on geometry of the lattice. If we can not neglect the interaction of a spin with the rest of the lattice, then we have *long-range models* for which it applies the general expression for the energy.

Now consider nearest-neighbor Ising models. We can assume for simplicity that all sites will react the same way to the external magnetic field, and that interactions will be isotropic. In this case the energy becomes

$$E(\boldsymbol{\sigma}) = -J \sum_{\langle ij \rangle} \sigma_i \sigma_j - h \sum_{i=1}^N \sigma_i \quad (3.5)$$

3.2.3 Noninteracting spins Ising model: exact solution

We suppose to have $J_{ij} = 0$. Then we have isolated spins immerse in an external field h . This is the model that we can use for a paramagnet. The hamiltonian becomes:

$$E(\boldsymbol{\sigma}) = -h \sum_{i=1}^N \sigma_i \quad (3.6)$$

This problem has an exact solution, because we can construct the partition function

$$Z(h, T) = \left(e^{h/(k_B T)} + e^{-h/(k_B T)} \right)^N = \left[2 \cosh \left(\frac{h}{k_B T} \right) \right]^N \quad (3.7)$$

and the Helmholtz free energy

$$A(h, T) = -k_B T \ln Z = -N k_B T \ln \left[2 \cosh \left(\frac{h}{k_B T} \right) \right] \quad (3.8)$$

Therefore we can study the thermodynamic of the system. The entropy turns out to be

$$S(h, T) = -\frac{\partial A}{\partial T} = N k_B \left(\ln \left[2 \cosh \left(\frac{h}{k_B T} \right) \right] - \frac{h}{k_B T} \tanh \left(\frac{h}{k_B T} \right) \right) \quad (3.9)$$

We note that the entropy of the system is vanishingly small for $k_B T \ll h$; it rises rapidly when $k_B T$ is of the order of h and approaches the limiting value $N k_B \ln(2)$ for $k_B T \gg h$. This limiting value of S corresponds to the fact that at high temperatures the orientation of the spins assumes a completely random character, with the result that the system now has 2^N equally likely micro states available to it.

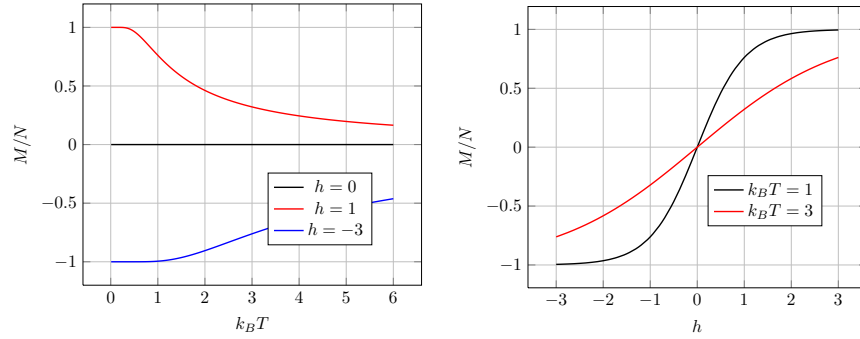


Figure 3.1: Noninteracting spins magnetization per spin.

Finally we can deduce the internal energy, the magnetization and the specific heat

$$U(h, T) = -T^2 \frac{\partial}{\partial T} \left(\frac{A}{T} \right) = -Nh \tanh \left(\frac{h}{k_B T} \right) \quad (3.10)$$

$$M(h, T) = -\frac{\partial A}{\partial h} = N \tanh \left(\frac{h}{k_B T} \right) \quad (3.11)$$

$$C(h, T) = \frac{\partial U}{\partial T} = Nk_B \left(\frac{h}{k_B T} \right)^2 \operatorname{sech}^2 \left(\frac{h}{k_B T} \right) \quad (3.12)$$

Therefore from our model for a paramagnet we can gather that

- when external field is off, for all temperatures, the system has not proper magnetization, ie $M(0, T) = 0$;
- when we turn on the field for all temperatures the system magnetize itself and the GS is the microstate in which all spins are oriented in the field's direction;
- the system has no phase transition!

3.2.4 Nearest-neighbor Ising models: mean field approximation

Very few models of statistical mechanics have been solved exactly (the ferromagnetic nearest-neighbor Ising model has been exactly solved in 1D and 2D); in most of the cases one has to rely on approximate methods. Among them, the mean-field approximation is one of the most widely used. The advantage of the mean-field theory (MFT) is its simplicity and that it correctly predicts the qualitative features of a system in most cases; so in general it is the first instrument one resorts to when exploring new models. The essence of the mean-field theory is the assumption of statistical independence of the local ordering (spins in the case of magnetic systems). The interaction terms in the Hamiltonian are replaced by an effective, “mean field” term. In this way, all the information on correlations in the fluctuations is lost.

Let us suppose that we mentally isolate a spin (which we will denote by the subscript k) from its environment, in the nearest-neighbor Ising model. If the spin's state changes from σ_k to σ'_k , while all the rest of the environment remains constant, the system's energy varies by

$$\Delta E = \left(-J \sum_{\langle ik \rangle} \sigma_i - h \right) \Delta \sigma_k \quad (3.13)$$

where $\Delta \sigma_k = \sigma'_k - \sigma_k$, and the sum is extended to the nearest-neighbor sites of k . This situation corresponds to a single magnet immersed in a field

$$J \sum_{\langle ik \rangle} \sigma_i + h \quad (3.14)$$

But nearest-neighbor spins fluctuate so we can imagine that our isolate spin interacts with an external efficace field defined by the mean

$$h^{\text{eff}} =: J \sum_{\langle ik \rangle} \langle \sigma_i \rangle + h \quad (3.15)$$

Thanks to MFT we have simplified the problem: indeed we know the thermodynamic for an isolated spin σ , subjected to an arbitrary external field h (see. *Noninteracting spins Ising model: exact solution*). We have a magnetization for spin equal to (3.11)

$$\langle \sigma \rangle = \frac{M}{N} = \tanh \left(\frac{h}{k_B T} \right) \quad (3.16)$$

By exploiting this result, and substituting h with h^{eff} , so we obtain for a nearest-neighbor Ising model

$$\langle \sigma_k \rangle = \tanh \left[\frac{1}{k_B T} \left(J \sum_{\langle ik \rangle} \langle \sigma_i \rangle + h \right) \right] \quad (3.17)$$

To go ahead from this point, now we need to work with ferromagnetic models. If we work with these we can suppose that the mean value of σ_k be the same for all spins. We can't do that if we use antiferromagnetic models! Thus

$$\langle \sigma_k \rangle =: m \quad \forall k \quad (3.18)$$

from which we obtain an equation for m (Bragg-Williams equation)

$$m = \tanh \left[\frac{1}{k_B T} (J\gamma m + h) \right] \quad (3.19)$$

We can solve that equation graphically.

3.2.5 Ferromagnetic nearest-neighbor Ising model: analytical solutions

In the previous section we solve ferromagnetic nearest-neighbor Ising models using MFT methods, that are dimension independent. However there are two systems that we can analyze using the direct partition function calculus: 1D ferromagnetic nearest-neighbor Ising model and 2D square lattice ferromagnetic zero-field nearest-neighbor Ising model. In this section we want to summarize historical results.

Let us consider 1D model. In the nearest neighbor case (with periodic or free boundary conditions) an exact solution is available. The energy of the one-dimensional Ising model on a lattice of N sites with periodic boundary conditions, such that the N^{th} spin becomes a neighbor of the first, is in a symmetrical form

$$H(\sigma) = -J \sum_{i=1}^N \sigma_i \sigma_{i+1} - h \sum_{i=1}^N \sigma_i \quad (3.20)$$

Using the transfer matrix method, first introduced by Kramers and Waanier in 1941, we can calculate easily the partition function. Then the free energy, in thermodynamical limit, is

$$A(\beta, h) = - \lim_{N \rightarrow \infty} \frac{1}{\beta N} \ln(Z(\beta)) = - \frac{1}{\beta} \ln \left(e^{\beta J} \cosh \beta h + \sqrt{e^{2\beta J} (\sinh \beta h)^2 + e^{-2\beta J}} \right) \quad (3.21)$$

The various other properties of the system follow readily from the Helmholtz free energy. For example, it is extremely important to consider the magnetization per spin:

$$m = \langle \sigma_k \rangle = \frac{\sinh(\beta h)}{\sqrt{e^{-4\beta J} + \sinh^2 \beta h}} \quad (3.22)$$

We note that, as $h \rightarrow 0$, $m \rightarrow 0$ for all finite temperatures. This rules out the possibility of spontaneous magnetization, and hence of a phase transition, at any finite temperature T . Mean Field approximation for the 1D ferromagnetic Ising model is wrong!

Of course, at $T = 0$, m (for any value of h) is equal to the saturation value 1, which implies perfect order in the system. This means that there is, after all, a phase transition at a critical temperature T_C , which coincides with absolute zero!

3.2.6 Lattice gas

The Ising model could apply equally well to a system of "occupied" and "unoccupied" lattice sites, i.e. to a system of "particles" and "holes" in a lattice, it was Yang and Lee who first used the term *lattice gas* to describe such a system [22]. By definition, a lattice gas is a collection of m atoms which can occupy only discrete positions in space-positions that constitute a lattice structure with a given coordination number. We associate an occupation number n_i ($i = 1, \dots, N$) to each site, that is either +1 if there is a particle in the site or 0 if the site is empty. The mapping from an Ising model to a lattice gas is:

$$n_i = \frac{1}{2}(\sigma_i + 1) \quad (3.23)$$

3.3 Ground States

3.3.1 Introduction

Until now we studied models with translational-invariant short-range interactions. We saw that, if we work with ferromagnetic Ising Models (IM), we can describe thermodynamical properties of the system, calculating the partition function. This step implies not trivial knowledge of system's microstate and their energy or energy levels and their degeneracy. When we don't know this structure we try to approximate it with MFT or other methods. But what about antiferromagnetic IM? And what about translational-invariant long-range interactions? We can't use previous techniques, so we need to start our study from something simpler.

The first step in a study of such IM amounts to understand low-temperature properties. Usually determining system's ground states (GS) represents the first problem in this case. Provided that the underlying interactions are short-range, numerous methods of searching for GS configurations are available. In the case of one-dimensional lattice systems, there is even an algorithmic method [23]. In higher dimensions, let us mention the powerful method of m -potential which is successful in many cases of interest.

However, if the translation-invariant interactions are long-range ones, the situation is drastically different. Rigorous results are scarce. To the best of our knowledge there exist only two kinds of interactions for which rigorous results have been obtained:

1. a version of one-dimensional Frenkel-Kontorova model [24];
2. a one-dimensional lattice-gas model with strictly convex repulsive two-body interactions [25].

Let us study Hubbard GS.

3.3.2 Hubbard ground-states

In his paper Hubbard [2] studied orderings of electrons in quasi-one-dimensional conductors. Starting from this system it emerged a 1D lattice-gas model, equivalent to a certain one-dimensional Ising model, for which Hubbard described a method of determining the exact GS when electrostatic interactions between electrons were dominant.

Let us suppose to have one-dimensional chain of N sites, that is our lattice Λ . We associate an occupation number n_i ($i = 1, \dots, N$) to each site, that is either +1 if there is a particle in the site or 0 if the site is empty. A vector $\mathbf{n} = \{n_i\}$ defines one system's configuration (microstate) as in table (3.1). There are 2^N possible configurations. We assume that particles interact only through two-body forces and to a pair of particles at lattice sites i and j , whose distance is $|i - j|$, we assign the translation-invariant interaction energy $V_{ij} = V_{ji} = V_{|i-j|} := V(|i - j|)$. The corresponding two-body potential reads $V(|i - j|)n_i n_j$. We can have only one particle for site and particles can't interact with themselves. In terms of the above defined potential, the Hubbard hamiltonian of our system amounts:

$$E(\mathbf{n}) = \frac{1}{2} \sum_{i=1}^N \sum_{j \neq i} V(|i - j|) n_i n_j \quad (3.24)$$

$\{n_i\}$	configuration												
0000000000000	○	○	○	○	○	○	○	○	○	○	○	○	○
1001000001010	●	○	○	○	○	○	○	○	○	○	○	○	○
0100110100110	○	●	○	○	○	○	○	○	○	○	○	○	○
⋮													
1111111111111	●	●	●	●	●	●	●	●	●	●	●	●	●

Table 3.1: Examples of microscopic configurations for a chain of 13 sites

We want to obtain the GS particle configurations of this model, i.e. to find the vector $\mathbf{n} = \{n_i\}$ that minimize Hubbard hamiltonian, supposing to fix particles' number m , i.e. in canonical ensemble. Therefore we have the condition on particles' number:

$$m =: \sum_{i=1}^N n_i \quad (3.25)$$

We can define also the filling factor (or particle density) $\rho := m/N$. There are $\binom{N}{m}$ possible configurations for $\mathbf{n} = \{n_i\}$, fixing ρ . The simplest intuitive consideration to allocate particles, since the potential is repulsive, is that objects are distributed as far as possible from each other, respecting restrictions imposed on their locations by the underlying lattice. Hubbard solved analitically that problem for an infinite chain and for a particular class of potentials, those satisfying the two conditions:

$$V(r) \rightarrow 0 \quad \text{as } r \rightarrow \infty \quad (3.26)$$

$$V(r+1) + V(r-1) \geq 2V(r) \quad \text{for all } r > 1 \quad (3.27)$$

Second conditions means that potential must be convex. It is satisfied for example by ordinary Coulomb potential and also by $V(|i-j|) = |i-j|^{-\alpha}$ where $\alpha > 0$. We now describe Hubbard solutions, called the *generalized Wigner lattices* or *most uniform configuration*, that are independent of any further details of the interaction potential.

Let us imagine our finite N -site chain deformed into an infinite chain of $N' \gg N$ sites with $\rho N'$ particles. We reduce the search area to ground states solutions that are N -periodic with ρN particles. Doing that we are forcing periodic boundary conditions (pbc) to our model:

$$n_{i+N} =: n_i \quad i = 1, \dots, N \quad (3.28)$$

that directly implies a new bond

$$\sum_{i=j}^{N+j} n_i = m \quad \forall j \quad (3.29)$$

So we consider the N -site chain deformed into a N -site loop: one N -site chain interacts with an infinite number of copies of itself. At each complete rotation on the ring corresponds to a movement of a period on the infinite chain. Doing that approximation we can describe our system in a simpler way.

Now let us label particles in order round the loop with an index $\nu = 1, \dots, m$ and let us define $r_\nu^{(0)}$ the position of ν particle and $r_\nu^{(1)}$ the interval between particle ν and $\nu+1$, so $r_\nu^{(1)} =: r_{\nu+1}^{(0)} - r_\nu^{(0)}$. Note that, because of pbc, we can obtain position of a generic particle on the infinite chain, i.e. $r_{\nu+m}^{(0)} = r_\nu^{(0)} + N$. From that we can derive $r_{\nu+m}^{(1)} = r_\nu^{(1)}$. The lattice spacing is set to one, throughout. We can define also the distance between particle ν and $\nu + \mu$

$$r_\nu^{(\mu)} =: r_{\nu+\mu}^{(0)} - r_\nu^{(0)} = \sum_{\tau=\nu}^{\nu+\mu-1} r_\tau^{(1)} = \sum_{\tau=0}^{\mu-1} r_{\nu+\tau}^{(1)} \quad (3.30)$$

From that we obtain useful properties

$$r_{\nu+m}^{(\mu)} = r_\nu^{(\mu)} \quad \text{for all } \mu \quad (3.31)$$

$$r_\nu^{(\mu+m)} = r_\nu^{(\mu)} + N \quad \text{for all } \mu \quad (3.32)$$

$\{n_i\}$	configuration												$\{r_\nu^{(1)}\}$	
1111100000000	●	●	●	●	●	○	○	○	○	○	○	○	○	$\{1,1,1,1,9\}$
1001001001010	●	○	○	●	○	○	●	○	○	●	○	●	○	$\{3,3,3,2,2\}$
00001101001110	○	○	○	○	●	●	○	●	○	○	●	●	○	$\{1,2,3,1,6\}$
⋮	⋮	⋮	⋮	⋮	⋮	⋮	⋮	⋮	⋮	⋮	⋮	⋮	⋮	⋮
1010010100100	●	○	●	○	○	●	○	●	○	○	●	○	○	$\{2,3,2,3,3\}$

Table 3.2: Examples of microscopic configurations for a loop of $N = 13$ sites, $\rho = 5/13$

Since energy is rotational invariant on the loop, it depends only on $\{r_\nu^{(\mu)}\}$, i.e. only relative position are fundamental. Therefore a vector $\mathbf{r}^{(1)} =: \{r_\nu^{(1)}\}$ defines one system's configuration (microstate) and satisfies $\sum_{\nu=1}^m r_\nu^{(1)} = N$. Note that $\mathbf{s}^{(1)} =: \{s_\nu^{(1)}\}$ where $s_\nu^{(1)} =: r_{\nu+1}^{(1)}$ identifies the same configuration of $\mathbf{r}^{(1)}$. So $\mathbf{r}^{(1)}$ defines one system's configuration less than transformations like $r_\nu^{(1)} \rightarrow r_{\nu+\tau}^{(1)}$ and one microstate satisfies $\sum_{\nu=\tau}^{m+\tau} r_\nu^{(1)} = N$ that implies $\sum_{\nu=\tau}^{m+\tau} r_\nu^{(\mu)} = \mu N$. Counting number of possible configurations with ρN particles on N sites on a ring it isn't a trivial problem (see Necklace, combinatory).

How can we express energy (3.24) in term of $\mathbf{r}^{(1)}$? The interaction energy between ν particle and $\nu + \mu$ particle is $V(r_\nu^{(\mu)})$; therefore the interaction energy between ν particle and the universe is

$$\sum_{\mu} V(r_\nu^{(\mu)}) = \sum_{\mu=1}^m V(r_\nu^{(\mu)}) + \sum_{\mu=m+1}^{2m} V(r_\nu^{(\mu)}) + \sum_{\mu=2m+1}^{3m} V(r_\nu^{(\mu)}) + \dots \quad (3.33)$$

$$= \sum_{\mu=1}^m V(r_\nu^{(\mu)}) + \sum_{\mu=1}^m V(r_\nu^{(\mu+m)}) + \sum_{\mu=1}^m V(r_\nu^{(\mu+2m)}) + \dots \quad (3.34)$$

$$= \sum_{\mu=1}^m \left(V(r_\nu^{(\mu)}) + V(r_\nu^{(\mu+m)}) + V(r_\nu^{(\mu+2m)}) + \dots \right) \quad (3.35)$$

$$= \sum_k \sum_{\mu=1}^m V(r_\nu^{(\mu+km)}) \quad (3.36)$$

that we can simplify using property (3.32)

$$\sum_{\mu} V(r_\nu^{(\mu)}) = \sum_k \sum_{\mu=1}^m V(r_\nu^{(\mu)} + kN) \quad (3.37)$$

To obtain energy of the system we have to sum energies of all particles

$$E(\mathbf{r}^{(1)}) = \frac{1}{2} \sum_{\nu} \sum_{\mu} V(r_\nu^{(\mu)}) \quad (3.38)$$

$$= \frac{1}{2} \sum_{\nu=1}^m \sum_k \sum_{\mu=1}^m V(r_\nu^{(\mu)} + kN) + \frac{1}{2} \sum_{\nu=m+1}^{2m} \sum_k \sum_{\mu=1}^m V(r_\nu^{(\mu)} + kN) + \dots \quad (3.39)$$

$$= \frac{1}{2} \sum_{\nu=1}^m \sum_k \sum_{\mu=1}^m V(r_\nu^{(\mu)} + kN) + \frac{1}{2} \sum_{\nu=1}^m \sum_k \sum_{\mu=1}^m V(r_{\nu+m}^{(\mu)} + kN) + \dots \quad (3.40)$$

$$= \frac{1}{2} \sum_{k,t} \sum_{\nu=1}^m \sum_{\mu=1}^m V(r_{\nu+tm}^{(\mu)} + kN) \quad (3.41)$$

that we can simplify using property (3.31) resulting Hubbard hamiltonian for an infinite chain with pbc

$$E(\mathbf{r}^{(1)}) = A \sum_k \sum_{\nu=1}^m \sum_{\mu=1}^m V(r_\nu^{(\mu)} + kN) = A \sum_k \sum_{\mu=1}^m U^k(\mathbf{r}^{(\mu)}) \quad (3.42)$$

where A it is a multiplicative factor (that depends on length of the chain). We have defined $\mathbf{r}^{(\mu)} =: \{r_\nu^{(\mu)}\}$ and

$$U^k(\mathbf{r}^{(\mu)}) =: \sum_{\nu=1}^m V(r_\nu^{(\mu)} + kN) \quad (3.43)$$

We have now basic ingredients to engage the problem. Our initial purpose was to look for an algorithm to minimize (3.42) with the condition

$$\sum_{\nu=1}^m r_\nu^{(1)} = N \quad (3.44)$$

This problem is similar to other m problems in which we minimize each inner sum (3.43) separately, each one with the condition

$$\sum_{\nu=1}^m r_\nu^{(\mu)} = \mu N \quad (3.45)$$

We know that if such solution exists it will also minimize (3.42). To obtain the solution for inner problems we need the following theorem.

Theorem 3.3.1. *If $\{r_i\} = r_1, \dots, r_m$ is a set of m integers such that*

$$\sum_{i=1}^m r_i := R = mr + a \quad \text{where } 0 \leq a < m \quad (3.46)$$

and if $V : \mathbb{N} \mapsto \mathbb{Z}$ is an integer function such that it is strictly convex, then

$$(m - a)V(r) + aV(r + 1) \leq \sum_{i=1}^m V(r_i) \quad (3.47)$$

Proof. First we suppose that $\{r_i\}$ is a set such that $|r_i - r_j| \leq 1$ for all pairs i, j ; such a set will be called *minimal*. We define $\hat{r} =: \min(r_i)$. For a minimal set we have $\hat{r} \leq r_i \leq \hat{r} + 1$ for all i : r_i can assume only value \hat{r} or $\hat{r} + 1$. Therefore we define \hat{n} as the “number of r_i that assumes value \hat{r} ”. Simultaneously $m - \hat{n}$ is the “number of r_i that assumes value $\hat{r} + 1$ ”. Calculating

$$\sum_{i=1}^m r_i = \hat{n}\hat{r} + (m - \hat{n})(\hat{r} + 1) = m\hat{r} + m - \hat{n} \quad (3.48)$$

for the uniqueness of the modular scomposition, we obtain $\hat{r} \equiv r$ and $m - \hat{n} \equiv a$. So it follows at once for minimal sets from (3.46) that the equality in (3.47) is satisfied.

Now let C be a non minimal set $\{r_i\}$, so for some $s \neq t$ one has $r_s > r_t + 1$. We construct the set C' taking C and moving only r_s and r_t

$$\begin{aligned} r'_i &=: r_i && \text{for all } i \neq s, t \\ r'_s &=: r_s - 1 \\ r'_t &=: r_t + 1 \end{aligned}$$

We see that C' satisfy the condition (3.46), and, using the lemma (3.3.2), we obtain

$$V(r'_t) + V(r'_s) \leq V(r_s) + V(r_t) \quad \Rightarrow \quad \sum_{i=1}^m V(r'_i) \leq \sum_{i=1}^m V(r_i) \quad (3.49)$$

If C' isn't minimal we repeat the procedure to obtain a C'' with

$$\sum_{i=1}^m V(r''_i) \leq \sum_{i=1}^m V(r'_i) \leq \sum_{i=1}^m V(r_i) \quad (3.50)$$

and so until one arrives at minimal set C^0 . Using inequalities between C^0, \dots, C one has the thesis

$$(m - a)V(r) + aV(r + 1) = \sum_{i=1}^m V(r_i^0) \leq \sum_{i=1}^m V(r_i) \quad (3.51)$$

□

Lemma 3.3.2. *Let $V : \mathbb{N} \mapsto \mathbb{Z}$ an integer function such that it is strictly convex i.e.*

$$V(r+1) + V(r-1) \geq 2V(r) \quad \text{for all } r > 1 \quad (3.52)$$

then

$$V(s+1) + V(t-1) \leq V(s) + V(t) \quad \text{for all } s \text{ such that } s < t \quad (3.53)$$

Proof. Starting from (3.52) and substituting $r' = r-1$ to r we obtain

$$V(r'+2) + V(r') \geq 2V(r'+1) \quad \text{for all } r' > 0 \quad (3.54)$$

Summing $V(r'-1)$ to both members and using (3.52) we obtain

$$\begin{aligned} V(r'+2) + \cancel{V(r')} + V(r'-1) &\geq 2V(r'+1) + V(r'-1) \\ &\geq V(r'+1) + \cancel{2V(r')} \end{aligned}$$

that fabricates a new disequation

$$V(r+2) + V(r-1) \geq V(r+1) + V(r) \quad \text{for all } r > 0 \quad (3.55)$$

We can use (3.55) as we manipulate (3.52) obtaining

$$V(r'+3) + V(r') \geq V(r'+2) + V(r'+1) \quad \text{for all } r' > -1 \quad (3.56)$$

and from that

$$\begin{aligned} V(r'+3) + \cancel{V(r')} + V(r'-1) &\geq V(r'+2) + V(r'+1) + V(r'-1) \\ &\geq V(r'+2) + \cancel{2V(r')} \end{aligned}$$

that fabricates a new disequation

$$V(r+3) + V(r-1) \geq V(r+2) + V(r) \quad \text{for all } r > -1 \quad (3.57)$$

We can iterate the initial algorithm, obtaining, at the k -th step

$$V(r+k+1) + V(r-1) \geq V(r+k) + V(r) \quad \text{for all } r > -k+1 \quad (3.58)$$

from which, naming $r-1 := s$ and $r+k+1 := t$, we demonstrate the thesis. \square

We demonstrate that, if $\{r_\nu^{(\mu)}\}$ it is a minimal set, it minimize energy (3.43). We need to fabricate that set. Starting from (3.45), we can calculate integers $r^{(\mu)}$ and $a^{(\mu)}$, decomposing the mixed fraction μ/ρ into the sum of a non-zero integer and a proper fraction:

$$\sum_{\nu=1}^m r_\nu^{(\mu)} = \mu N = mr^{(\mu)} + a^{(\mu)} \quad \Rightarrow \quad \frac{\mu}{\rho} = r^{(\mu)} + \frac{a^{(\mu)}}{m} \quad (3.59)$$

We obtain that $r^{(\mu)} = \lfloor \mu/\rho \rfloor$. So if $r_\nu^{(\mu)} \in S^\mu(\rho) := [r^{(\mu)}, r^{(\mu)} + 1] = [\lfloor \mu/\rho \rfloor, \lfloor \mu/\rho \rfloor + 1]$ then $\{r_\nu^{(\mu)}\}$ it is a minimal set. There are $m - a^{(\mu)}$ of $r_\nu^{(\mu)}$ that take value $\lfloor \mu/\rho \rfloor$ and $a^{(\mu)}$ of $r_\nu^{(\mu)}$ that take value $\lfloor \mu/\rho \rfloor + 1$.

Therefore a set of solution that minimize (3.43) exists for each $\mu = 1, \dots, m$; so, for all fixed ρ , energy (3.42) is minimized when $r_\nu^{(\mu)} \in S^\mu(\rho)$ for each $\mu = 1, \dots, m$.

Example 3.3.1. *Let us take $m = 5$ and $N = 13$ then $\rho = 5/13$. Calculating $r^{(\mu)}$ and $a^{(\mu)}$ we obtain minimal configuration for each μ . Results are in the following table.*

Note that each set of $r_\nu^{(\mu)}$ minimize energy (3.43) independently from the internal order of numbers. For example both $\{2, 2, 3, 3, 3\}$ and $\{2, 3, 2, 3, 3\}$ minimize $U(\mathbf{r}^{(1)})$. But from $\{r_\nu^{(1)}\} = \{2, 2, 3, 3, 3\}$ it descend the $\{r_\nu^{(2)}\}$ configuration $\{4, 5, 6, 6, 5\}$ that is not minimal set for $U(\mathbf{r}^{(2)})$.

¹ $\lfloor x \rfloor$ means integer part of x

μ	$r^{(\mu)}$	$m - a^{(\mu)}$	$r^{(\mu)} + 1$	$a^{(\mu)}$	$\{r_\nu^{(\mu)}\}$
1	2	2	3	3	{2,2,3,3,3}
2	5	4	6	1	{5,5,5,5,6}
3	7	1	8	4	{7,8,8,8,8}
4	10	3	11	2	{10,10,10,11,11}
5	13	5	14	0	{13,13,13,13,13}

Table 3.3: Minimal sets for U , $m = 5$ and $N = 13$

Therefore to minimize energy (3.42) we need to combine results in table and to choose only one $\{r_\nu^{(1)}\}$ configuration, i.e. to specify the $r_\nu^{(1)}$ ordering, for less than rotations.

In our example we have only two fundamental configuration. They generate the chain of configurations

$$\begin{aligned} \{2, 2, 3, 3, 3\} &\rightarrow \{4, 5, 6, 6, 5\} \rightarrow \{7, 8, 9, 8, 7\} \rightarrow \{10, 11, 11, 10, 10\} \rightarrow \{13, 13, 13, 13, 13\} \\ \{2, 3, 2, 3, 3\} &\rightarrow \{5, 5, 5, 6, 5\} \rightarrow \{7, 8, 8, 8, 8\} \rightarrow \{10, 11, 10, 11, 10\} \rightarrow \{13, 13, 13, 13, 13\} \end{aligned}$$

so the configuration that minimize total energy is $\{r_\nu^{(1)}\} = \{2, 3, 2, 3, 3\}$ that we call most uniform configuration for $\rho = 5/13$. We can write this result using compact notation, illustrate later

$$\{2, 3, 2, 3, 3\} =: (10100)^2(100) = (23)^2(3)$$

We have demonstrate that, for each μ exists a set of microstates that minimize $U(\mathbf{r}^{(\mu)})$ and we know how to construct it. We don't have a method to choice one of these configurations that minimizes total energy (3.42) yet, but we can fabricate it. We start using $\mu = 1$, i.e. we want to minimize nearest-neighbor energy $U(\mathbf{r}^{(1)})$. We obtain our set of minimal configurations applying the algorithm of the theorem. We calculate $r^{(1)}$ and $a^{(1)}$ from the decomposition

$$\frac{1}{\rho} = r^{(1)} + \frac{a^{(1)}}{m} \quad (3.60)$$

and then we have the set of configurations that minimizes $U(\mathbf{r}^{(1)})$, i.e. $\{r_\nu^{(1)}\}$ such that there are $m - a^{(1)}$ times $r^{(1)}$ and $a^{(1)}$ times $r^{(1)} + 1$. For example, if $a^{(1)} = 0$, i.e. $\rho = 1/r^{(1)}$ that is the simplest possibility, we have only one configuration that satisfy our problem: particles are distributed uniformly, one every $r^{(1)}$ sites. Indeed

$$\{r_\nu^{(1)}\}_{\rho=1/r^{(1)}} = \{r^{(1)}, r^{(1)}, \dots, r^{(1)}\} \quad (3.61)$$

This microstate solves also the general problem, as we can verify comparing the chain of configurations that our solution generates with sets of configurations that minimize $U(\mathbf{r}^{(\mu)})$.

$$\{r^{(1)}, r^{(1)}, \dots, r^{(1)}\} \rightarrow \{r^{(2)} = 2r^{(1)}, r^{(2)}, \dots, r^{(2)}\} \rightarrow \dots \quad (3.62)$$

Now let us introduce new notation to indicate our set of microstates that minimizes $U(\mathbf{r}^{(1)})$. An element $r_\nu^{(1)}$ can be $r^{(1)}$ or $r^{(1)} + 1$. To identify only one system's configuration we have to know the pattern of $r_\nu^{(1)}$ in the vector $\{r_\nu^{(1)}\}$, less than rotations. However, knowing that $r_\nu^{(1)} = r^{(1)}$ means that we have a grouping of particles and holes such that after particle ν we must have $r^{(1)} - 1$ holes. In term of occupation numbers when we find $r_\nu^{(1)}$ we fixe a part of configuration, that we indicate with round brackets. We have only two types of partial-configuration ($10^{(r^{(1)}-1)}$) and ($10^{(r^{(1)})}$). If we assume that particle is always at the beginning of the string, we can compact the notation for partial configuration, using ($10^{(r^{(1)}-1)}$) =: $(r^{(1)})$ or ($10^{(r^{(1)})}$) =: $(r^{(1)} + 1)$. Choice a configuration means fixing the order of partial configuration. Using that considerations a minimal configuration for $U(\mathbf{r}^{(1)})$ is part of

$$M_1 := \left\{ \{n_i\} : \begin{array}{l} (r^{(1)}) \times [m - a^{(1)}] \\ (r^{(1)} + 1) \times [a^{(1)}] \end{array} \right\} \quad (3.63)$$

To understand the notation let us consider examples.

Example 3.3.2. Let us take $m = 5$ and $N = 13$ then $\rho = 5/13$. We obtain $r^{(1)} = 2$, so the partial configurations are (10) and (100). Minimal configurations for $U(\mathbf{r}^{(1)})$ are $\{2, 3, 2, 3, 3\} = (10)(100)(10)(100)(100) = (23)^2(3)$ and $\{2, 2, 3, 3, 3\} = (10)(10)(100)(100)(100) = (2)^2(3)^3$.

Example 3.3.3. Let us take $\rho = 1/n$ then $m = N/n$. We obtain $r^{(1)} = n$, so the partial configurations are (10^{n-1}) and (10^n) . Minimal configuration for $U(\mathbf{r}^{(1)})$ is $\{n, \dots, n\} = (10^{n-1})^m = (n)^m$.

Let us observe that the smallest possible partial configuration are (1) and (0), that we call 0-particles, so a generic system configuration is part of:

$$M_0 := \left\{ \{n_i\} : \begin{array}{l} (0) \times [N - m] \\ (1) \times [m] \end{array} \right\} \quad (3.64)$$

Knowing minimal sets for $U(\mathbf{r}^{(1)})$ (i.e. ρ density decomposition) permits a first ordering of 0-particles in bigger partial configurations $M_1 \subset M_0$:

$$\left\{ \{n_i\} : \begin{array}{l} (0) \times [N - m] \\ (1) \times [m] \end{array} \right\} \longrightarrow \left\{ \{n_i\} : \begin{array}{l} (r^{(1)}) \times [m - a^{(1)}] \\ (r^{(1)} + 1) \times [a^{(1)}] \end{array} \right\} \quad (3.65)$$

How we order partial configurations to obtain GS for (3.42), i.e how can we choice one microstate that minimize (3.42) between microstates (3.63) that minimize $U(\mathbf{r}^{(1)})$? If $a^{(1)} = 0$ we know the solution yet: we have only one configuration in the set (3.63) that is our GS. If $a^{(1)} \neq 0$ the second term $a^{(1)}/m$ in the ρ density decomposition represents the density of $(r^{(1)} + 1)$ sites intervals which can be regarded as defects, or particles, within the $(r^{(1)})$ sites intervals, which can be regarded as holes [26]. In that way we define two types of 1-particles. Therefore we want to find Hubbard GS for a density $\rho = a^{(1)}/m$ (why?, who are you minimizing?). We know which is the first step to solve this problem. We calculate $s^{(1)}$ and $b^{(1)}$ from the decomposition

$$\frac{m}{a^{(1)}} = s^{(1)} + \frac{b^{(1)}}{m} \quad (3.66)$$

Then, if $\{s_\nu^{(1)}\}$ is the vector of distance between 1-particles, i.e. it indicates how many $(r^{(1)})$ sites intervals there are between $(r^{(1)} + 1)$ sites intervals, we have $m - b^{(1)}$ of $s_\nu^{(1)}$ that are $s^{(1)}$ and $b^{(1)}$ of $s_\nu^{(1)}$ that are $s^{(1)} + 1$. So we obtain two type of 2-particles

$$((r^{(1)} + 1)(r^{(1)})(s^{(1)} - 1)) \quad ((r^{(1)} + 1)(r^{(1)})(s^{(1)})) \quad (3.67)$$

and a subsetset of M_1 that minimize also $U(\mathbf{r}^{(2)})$

$$M_2 := \left\{ \{n_i\} : \begin{array}{l} ((r^{(1)} + 1)(r^{(1)})(s^{(1)} - 1)) \times [m - b^{(1)}] \\ ((r^{(1)} + 1)(r^{(1)})(s^{(1)})) \times [b^{(1)}] \end{array} \right\} \quad (3.68)$$

If $b^{(1)} = 0$ we have only one configuration that is our solution. If $b^{(1)} \neq 0$ the second term $b^{(1)}/m$ in the $a^{(1)}/m$ density decomposition represents the density of (1) 2-particles within the (0) 2-particles. We can repeat the algorithm used before for 1-particles. And so on as long as when we find a null density fraction for k -particles. Indeed in that case we have only one configuration in M_k , that is GS.

Example 3.3.4. Let us take $m = 5$ and $N = 13$ then $\rho = 5/13$. We start from the set of 0-particles

$$M_0 := \left\{ \{n_i\} : \begin{array}{l} (0) \times [8] \\ (1) \times [5] \end{array} \right\} \quad (3.69)$$

From 5/13 decomposition we obtain the set of 1-particles

$$\frac{13}{5} = 2 + \frac{3}{5} \longrightarrow M_1 := \left\{ \{n_i\} : \begin{array}{l} (2) \times [2] \\ (3) \times [3] \end{array} \right\} \quad (3.70)$$

From 3/5 decomposition we obtain the set of 2-particles

$$\frac{5}{3} = 1 + \frac{2}{3} \longrightarrow M_2 := \left\{ \{n_i\} : \begin{array}{l} (3) \times [1] \\ (32) \times [2] \end{array} \right\} \quad (3.71)$$

From 2/3 decomposition we obtain the set of 3-particles

$$\frac{3}{2} = 1 + \frac{1}{2} \longrightarrow M_3 := \left\{ \{n_i\} : \begin{array}{l} (32) \times [1] \\ (323) \times [1] \end{array} \right\} \quad (3.72)$$

Finally from 1/2 decomposition we obtain the set of 4-particles

$$2 = 2 + \frac{0}{1} \longrightarrow M_4 := \{ \{n_i\} : (32332) \times [1] \} \quad (3.73)$$

Example 3.3.5. Let us take $m = 11$ and $N = 47$ then $\rho = 11/47^2$. We start from the set of 0-particles

$$M_0 := \left\{ \{n_i\} : \begin{array}{l} (0) \times [36] \\ (1) \times [11] \end{array} \right\} \quad (3.74)$$

From 11/47 decomposition we obtain the set of 1-particles

$$\frac{47}{11} = 4 + \frac{3}{11} \longrightarrow M_1 := \left\{ \{n_i\} : \begin{array}{l} (4) \times [8] \\ (5) \times [3] \end{array} \right\} \quad (3.75)$$

From 3/11 decomposition we obtain the set of 2-particles

$$\frac{11}{3} = 3 + \frac{2}{3} \longrightarrow M_2 := \left\{ \{n_i\} : \begin{array}{l} (544) \times [1] \\ (5444) \times [2] \end{array} \right\} \quad (3.76)$$

From 2/3 decomposition we obtain the set of 3-particles

$$\frac{3}{2} = 1 + \frac{1}{2} \longrightarrow M_3 := \left\{ \{n_i\} : \begin{array}{l} (5444) \times [1] \\ (5444544) \times [1] \end{array} \right\} \quad (3.77)$$

Finally from 1/2 decomposition we obtain the set of 4-particles

$$2 = 2 + \frac{0}{1} \longrightarrow M_4 := \{ \{n_i\} : (54445445444) \times [1] \} \quad (3.78)$$

Let us analyze some detail. First will the algorithm have an end? We observe that we are representing rational number ρ using a continued fraction. And we know that

Theorem 3.3.3. *Every finite continued fraction is a rational number, and each can be represented by a finite continued fraction in precisely two different ways.*

Second, what about $\rho = m/N = pm'/pN'$ if it isn't a lowest terms fraction (i.e. $p > 1$)? The GS configuration that we obtain considering m' particles on N' sites is the base for the GS periodic configuration of a system with pm' particles on pN' sites. Let us analyze the algorithm. We start from

$$M_0 = \left\{ \{n_i\} : \begin{array}{l} (0) \times [N - m] \\ (1) \times [m] \end{array} \right\} = \left\{ \{n_i\} : \begin{array}{l} (0) \times [N' - m'] \\ (1) \times [m'] \end{array} \times [p] \right\} = M'_0 \times [p] \quad (3.79)$$

From ρ decomposition we obtain

$$r'^{(1)} + \frac{a'^{(1)}}{m'} = \frac{1}{\rho} = r^{(1)} + \frac{a^{(1)}}{m} = r^{(1)} + \frac{a^{(1)}}{pm'} \Rightarrow \begin{array}{l} r^{(1)} = r'^{(1)} \\ a^{(1)} = pa'^{(1)} \end{array} \quad (3.80)$$

The second step is

$$M_1 = \left\{ \{n_i\} : \begin{array}{l} (r^{(1)}) \times [m - a^{(1)}] \\ (r^{(1)} + 1) \times [a^{(1)}] \end{array} \right\} = \left\{ \{n_i\} : \begin{array}{l} (r^{(1)}) \times [N' - m'] \\ (r^{(1)} + 1) \times [m'] \end{array} \times [p] \right\} = M'_1 \times [p] \quad (3.81)$$

Applying recursively the algorithm we find that, for GS,

$$M_k = \dots = M'_k \times [p] \quad (3.82)$$

²Hubbard example

This equation demonstrate that microstate M_k is the periodic repetition of M'_k , since M'_k contains only one configuration, and we have only one method to combine one object with itself. Indeed it is sufficient to obtain GS for simplified densities ρ , or densities in which numerator and denominator are coprime.

Finally we can further simplify the problem. Indeed it is sufficient to obtain the GS for $\rho \leq \frac{1}{2}$. To obtain the solution for any density ρ one have to calculate GS for $1 - \rho$ and interchange electrons and holes [26].

3.3.3 Hubbard algorithm

Let summarize Hubbard algorithm for a filling fraction ρ . We start representing ρ as a continued fraction,

$$\rho = \frac{1}{u_1 + \frac{1}{u_2 + \dots}} =: [0; u_1, \dots, u_k] \quad (3.83)$$

Then we define n -particles Y_n and n -holes X_n recursively

$$X_n := (Y_{n-1})(X_{n-1})^{u_n - 1} \quad (3.84)$$

$$Y_n := (Y_{n-1})(X_{n-1})^{u_n} \quad (3.85)$$

Our initial conditions are 0-particles and 0-holes

$$X_0 := (0) \quad (3.86)$$

$$Y_0 := (1) \quad (3.87)$$

Hubbard ground state is X_k .

ρ	X_k	configuration
$\frac{1}{3}$	(3)	● ○ ○ ● ○ ○ ● ○ ○ ● ○ ○ ● ○ ○ ● ⋯
$\frac{3}{7}$	(322)	● ○ ○ ● ○ ● ○ ● ○ ○ ● ○ ● ⋯
$\frac{5}{13}$	(32) ² (3)	● ○ ○ ● ○ ● ○ ○ ● ○ ● ○ ● ○ ○ ⋯

Table 3.4: Hubbard ground states

3.4 Phase transitions

Until now we have obtained periodic ground states for hamiltonian (3.24): fixing rational density (or filling fraction or particles number) corresponds to choose one ground state (up to translations) with that density of particles. From now on we want to study our system in grandcanonical ensemble, i.e. we want to change the particles number. If we used (3.24), we would have only one phase that is Hubbard ground state for $\rho = 0$, i.e. the system prefers to not have particles. Therefore we need to introduce a chemical potential (or an external field) $h > 0$ that forces our system to gain particles. We suppose that each site reacts in the same manner to external field, i.e. h doesn't depend on particle's position. So the Hamiltonian begins

$$E(\mathbf{n}) = -h \sum_{i=1}^N n_i + \frac{1}{2} \sum_{i=1}^N \sum_{j \neq i}^N V(|i-j|) n_i n_j \quad (3.88)$$

that is, if we consider Hubbard model, i.e. we have an infinite chain (chain of length N with periodic boundary conditions) and periodic configurations

$$E(\mathbf{r}^{(1)}) = A \left(-2hm + \sum_k \sum_{\mu=1}^m U^k(\mathbf{r}^{(\mu)}) \right) \quad (3.89)$$

For each value of h we have only one periodic ground state, or phase, that is part of Hubbard ground states. So, for each value of h we have an Hubbard configuration of density ρ . We can construct a ground state phase diagram in grandcanonical ensemble that is particle density versus the chemical potential of particles, $\rho(h)$. We are not able to calculate directly $\rho(h)$ but we can understand in which region of the parameter space, a given configuration of filling fraction $\rho = m/N$ is stable. We analyze the energy cost of inserting or extracting one excitation from a given configuration. If both operations increase the energy, the configuration is stable. The solution was given by Bak in [18].

3.4.1 Devil's staircase

Bak considered that the most interesting property of Hubbard ground states is the periodicity and studied its relation with a parameter. He argued that periodicity of a system tend to be commensurate with the lattice constant of the system. As a parameter is changed, the system may pass through several commensurate phases which may or may not have incommensurate phases between them. We know [27] that there are Ising models with an infinity of commensurate phases. At low temperatures there are only commensurate phases.

Therefore periodicity may assume every single commensurate (respect to lattice constant of the system) value in an interval, and rational numbers are everywhere dense, “two steps in the function showing the periodicity versus the parameter are then always separated by an infinity of more steps. This structure is called the devil's staircase. If the commensurate phases fill up the whole phase diagram the staircase is called complete”.

We now want to demonstate the existence of the complete devil's staircase for our Hubbard model. Let us calculate the region of the parameter space h in which Hubbard ground state for $\rho = m/N$ is stable. We suppose to inserting or extracting one excitation on pN sites, obtaining a Hubbard configuration with filling fraction $\rho' = pm + 1/pN$ or $\rho'' = pm - 1/pN$, where we have to find p such that we don't disturb too much the order, i.e. we are demanding that distances between particles change a little. So, our hypothesis are

$$\begin{cases} r^\mu(\rho') = \left\lfloor \frac{\mu p N}{pm+1} \right\rfloor = \left\lfloor \frac{\mu N}{m} \right\rfloor = r^\mu(\rho) & \forall \mu \pmod{m} = 1, \dots, m-1 \\ r^\mu(\rho') = \left\lfloor \frac{\mu p N}{pm+1} \right\rfloor = \left\lfloor \frac{\mu N}{m} \right\rfloor - 1 = kN - 1 & \forall \mu = km \end{cases} \quad (3.90)$$

$$\begin{cases} r^\mu(\rho'') = \left\lfloor \frac{\mu p N}{pm-1} \right\rfloor = \left\lfloor \frac{\mu N}{m} \right\rfloor = r^\mu(\rho) & \forall \mu \pmod{m} = 1, \dots, m-1 \\ r^\mu(\rho'') = \left\lfloor \frac{\mu p N}{pm-1} \right\rfloor = \left\lfloor \frac{\mu N}{m} \right\rfloor = kN & \forall \mu = km \end{cases} \quad (3.91)$$

where $r^\mu(\rho)/r^\mu(\rho')/r^\mu(\rho'')$ is the minimal distance that we obtain with Hubbard algorithm for $\rho/\rho'/\rho''$.

Since we know that all states are Hubbard kinds, we know the configurations structure. We know that we have $m - a^\mu(\rho)$ distances ($r^\mu(\rho)$) and $a^\mu(\rho)$ distances ($r^\mu(\rho) + 1$) for ρ ; we can suppose to have $m + 1 - a^\mu(\rho')$ distances ($r^\mu(\rho')$) and $a^\mu(\rho')$ distances ($r^\mu(\rho') + 1$) for ρ' and $m - 1 - a^\mu(\rho'')$ distances ($r^\mu(\rho'')$) and $a^\mu(\rho'')$ distances ($r^\mu(\rho'') + 1$) for ρ'' . Our second hypothesis is that all states satisfied Hubbard bond (we don't change the lenght of chain, when we change density):

$$\sum_{v=1}^{m(\rho)} r_v^\mu(\rho) = \mu N \quad (3.92)$$

then

$$\sum_{v=1}^m r_v^\mu(\rho) = \mu N = mr^\mu(\rho) + a^\mu(\rho) \quad (3.93)$$

$$\sum_{v=1}^{m+1} r_v^\mu(\rho') = \mu N = (m+1 - a^\mu(\rho'))r^\mu(\rho') + a^\mu(\rho')(r^\mu(\rho') + 1) = mr^\mu(\rho') + r^\mu(\rho') + a^\mu(\rho') \quad (3.94)$$

$$\sum_{v=1}^{m-1} r_v^\mu(\rho'') = \mu N = (m-1 - a^\mu(\rho''))r^\mu(\rho'') + a^\mu(\rho'')(r^\mu(\rho'') + 1) = mr^\mu(\rho'') - r^\mu(\rho'') + a^\mu(\rho'') \quad (3.95)$$

from which we obtain two equations

$$mr^\mu(\rho') + r^\mu(\rho') + a^\mu(\rho') = mr^\mu(\rho) + a^\mu(\rho) \quad (3.96)$$

$$mr^\mu(\rho'') - r^\mu(\rho'') + a^\mu(\rho'') = mr^\mu(\rho) + a^\mu(\rho) \quad (3.97)$$

Replacing values of $r^\mu(\rho')/r^\mu(\rho'')$ that we have hypothesized we calculate values of $a^\mu(\rho')/a^\mu(\rho'')$.

$$\begin{cases} a^\mu(\rho') = a^\mu(\rho) - r^\mu(\rho) & \forall \mu \pmod{m} = 1, \dots, m-1 \\ a^\mu(\rho') = m+1 - kN & \forall \mu = km \end{cases} \quad (3.98)$$

$$\begin{cases} a^\mu(\rho'') = a^\mu(\rho) + r^\mu(\rho) & \forall \mu \pmod{m} = 1, \dots, m-1 \\ a^\mu(\rho'') = kN & \forall \mu = km \end{cases} \quad (3.99)$$

Throughout, $r^\mu := r^\mu(\rho)$ and $a^\mu := a^\mu(\rho)$. Therefore inserting one excitation matches to transform Hubbard GS with $m - a^\mu$ distances (r^μ) and a^μ distances ($r^\mu + 1$) in Hubbard GS with $m - a^\mu + 1 + r^\mu$ distances (r^μ) and $a^\mu - r^\mu$ distances ($r^\mu + 1$); we are replacing r^μ distances ($r^\mu + 1$) by $r^\mu + 1$ distances (r^μ). With the same logic one understands that extracting excitation from the system will replace $r^\mu + 1$ distances (r^μ) by r^μ distances ($r^\mu + 1$). In a schematic way we can write:

	$\mu \pmod{m} = 1, \dots, m-1$	$\mu = km$	
$\rho \rightarrow$	$(r^\mu) \times m - a^\mu$ $(r^\mu + 1) \times a^\mu$	$(kN) \times m$	(3.100)
$\rho' \rightarrow$	$(r^\mu) \times m - a^\mu + 1 + r^\mu$ $(r^\mu + 1) \times a^\mu - r^\mu$	$(kN - 1) \times kN$ $(kN) \times m + 1 - kN$	
$\rho'' \rightarrow$	$(r^\mu) \times m - a^\mu - (1 + r^\mu)$ $(r^\mu + 1) \times a^\mu + r^\mu$	$(kN) \times m - 1 - kN$ $(kN + 1) \times kN$	

If we evaluate the energy on an Hubbard ground state we have

$$E(\rho) = -2hm + \sum_{k=1}^{\infty} \sum_{\mu=1}^m (m - a^\mu)V(r^\mu + kN) + a^\mu V(r^\mu + kN + 1) \quad (3.101)$$

that directly depends on number of particles m .

Until now, starting from a given ρ configuration, we have constructed two Hubbard phases ρ' and ρ'' with which comparing it. Now we have all the ingredients to obtain the energy difference between ρ' GS and ρ GS (inserting excitation):

$$\begin{aligned} \Delta E_+ &= E(\rho') - E(\rho) = \\ &= -2h_+ + \sum_{k=1}^{\infty} \sum_{\mu=1}^{m-1} (r^\mu + kN + 1)V(r^\mu + kN) - (r^\mu + kN)V(r^\mu + kN + 1) + \\ &+ \sum_{k=1}^{\infty} (1 - kN)V(kN) + (kN)V(kN - 1) \end{aligned} \quad (3.102)$$

and similarly the energy difference between ρ'' GS and ρ GS (extracting excitation):

$$\begin{aligned}\Delta E_- &= E(\rho'') - E(\rho) = \\ &= 2h_- - \sum_{k=1}^{\infty} \sum_{\mu=1}^{m-1} (r^\mu + kN + 1)V(r^\mu + kN) - (r^\mu + kN)V(r^\mu + kN + 1) + \\ &\quad + \sum_{k=1}^{\infty} (kN)V(kN + 1) - (1 + kN)V(kN)\end{aligned}\tag{3.103}$$

The interval in h , $\Delta h(\rho) = h_+ - h_-$, where the ground state is stable is determined simply by setting (3.102) and (3.103) equal to zero, because we want that $\Delta E_+ \geq 0$ for all ρ' and $\Delta E_- \geq 0$ for all ρ'' ; respectively

$$\frac{1}{2}\Delta h = \sum_{k=1}^{\infty} (kN) [V(kN + 1) + V(kN - 1) - 2V(kN)]\tag{3.104}$$

Note that $\Delta h(\rho)$ is independent of the numerator m and it is intensive. Sinai studied that problem in an analytical way [28], obtaining the same result.

Using that analytical formula we can plot the phase diagram for (3.89) with a strictly convex potential. We have to choose one fundamental energy, that is our minimum distinguishable value to calculate. How we do that? We assume that exist some density $\rho_0 = 1/N$ that is stable for $h = 0$, with high N . The energy of $\rho_0 = 1/N$ it is our energy quantum.

Now we construct the phase diagram. We suppose $h_-(\rho_0) = 0$. We calculate $h_+(\rho_0)$ using (3.104) with a larger number of term. Now we flip one spin up, because over $h_+(\rho_0)$, the phase ρ_0 isn't stable. So we consider $\rho_1 = 2/N$ and we fix $h_-(\rho_1) := h_+(\rho_0)$. We calculate $h_+(\rho_1) = 2/N$ stability interval and so on. The algorithm to construct phase diagram is recursive. Choosing one fundamental energy means fixing the N value, that we have first to choose. Our initial conditions are:

$$\begin{cases} \rho_0 := \frac{1}{N} \\ h_-(\rho_0) := 0 \end{cases}\tag{3.105}$$

then we have to apply recursively:

$$\begin{cases} h_+(\rho_i) := h_-(\rho_i) + \Delta h(\rho_i) \\ \rho_{i+1} := \rho_i + \frac{1}{N} \\ h_-(\rho_{i+1}) := h_+(\rho_i) \end{cases}\tag{3.106}$$

Results are in Figure (3.2) and (3.3).

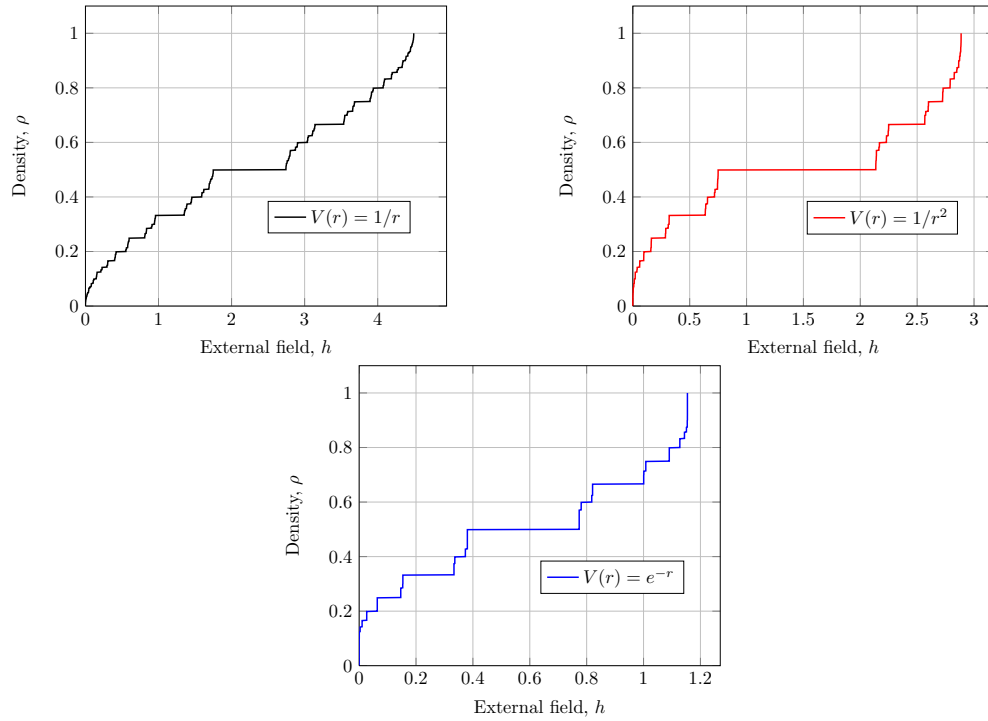


Figure 3.2: Phase diagram with the *Devil's staircase* for different potentials. The density of particle ρ is plotted vs the applied field h . It emerges its fractal and recursive structure.

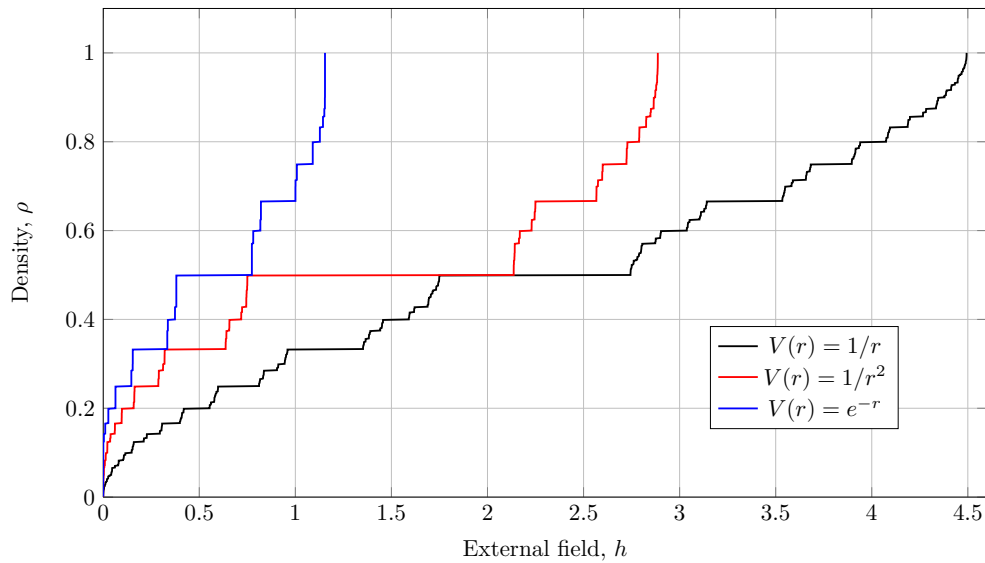


Figure 3.3: Comparison between the phase diagrams. We observe that the longest plateau ever corresponds to $\rho = 1/2$; then there are $1/3$ and $2/3$. It is observed that stronger potentials wear the system in saturation more quickly. Another interesting feature emerges by comparing the length of the plateau at $1/2$ between $1/r^\alpha$ potentials: the length increases as the parameter enhances.

Conclusions

In this paper we describe a tentative microscopic description of the fractional quantum Hall effect, that is inspired but different from the Tao-Thouless approach. Starting from the hamiltonian of interacting electrons in magnetic field, we elaborate and develop the idea that the microscopic mechanism behind the fractional quantization of the “filling fraction” (which is assumed to be related to the Hall conductivity) may be a collective phenomenon resulting from the electron repulsion.

In particular, starting from TT Coulomb matrix element, we map the quantum Hall hamiltonian in the thermodynamic limit and in momentum space, to Bak’s hamiltonian for a lattice gas with long-range repulsive interaction. Since the properties of the latter are known, we obtain that the phase diagram, i.e. the filling fraction versus magnetic field $\nu(B)$, has plateaux with fractal structure similar to the experimental plots of Hall’s conductivity $\sigma_{xy}(B)$. However there are important differences between the two physical quantities, which still require a full comprehension of the link between filling fractions and conductivity. Through our model, we think that we can also obtain an explicit second-quantized form for hamiltonian eigenstates, that are Hubbard’s ground-states in momentum space.

What about the future? In order to give a quantitative measure of the effectiveness of the model it would be necessary:

- to understand the origin of TT Coulomb matrix element, and to generalize it by introducing an external electric field \mathbf{E} . This step should permit to evaluate the Hall conductivity as the ratio of the electric field and the mean value of the current density on our hamiltonian ground states and to understand its connection with filling fractions;
- to write Laughlin ansatz in second quantization form, and evaluate its overlap with our hamiltonian eigenstates and;
- to understand how the deviations of the potential \tilde{V} , obtained in momentum space, from the assumptions of Bak’s model change results.

A lot of relevant topics remain to be developed before we can satisfactorily end the discussion on this work.

Acknowledgements

I would like to thank all the people who contributed in some way to the work described in this thesis. First and foremost, I would like to express my gratitude to my supervisors, Luca Molinari and Pietro Rotondo. Moreover I would like to thank my father, Alessandro, because he has always shown interest in my work. Finally, I would like to acknowledge friends and family who supported me during my time here.

Bibliography

- [1] R. Tao and D. J. Thouless, “Fractional quantization of hall conductance,” *Phys. Rev. B*, vol. 28, pp. 1142–1144, Jul 1983.
- [2] J. Hubbard, “Generalized wigner lattices in one dimension and some applications to tetracyanoquinodimethane (tcnq) salts,” *Phys. Rev. B*, vol. 17, pp. 494–505, Jan 1978.
- [3] D. J. Thouless, “Long-range order and the fractional quantum hall effect,” *Phys. Rev. B*, vol. 31, pp. 8305–8307, Jun 1985.
- [4] R. B. Laughlin, “Anomalous quantum hall effect: An incompressible quantum fluid with fractionally charged excitations,” *Phys. Rev. Lett.*, vol. 50, pp. 1395–1398, May 1983.
- [5] D. Yoshioka, *The Quantum Hall Effect*. Springer Berlin Heidelberg, 2002.
- [6] Z. F. Ezawa, *Quantum Hall Effects: Recent Theoretical and Experimental Developments (3rd ed.)*. World Scientific, 2013.
- [7] E. H. Hall, “On a new action of the magnet on electric currents,” *American Journal of Mathematics*, vol. 2, no. 3, pp. pp. 287–292, 1879.
- [8] D. C. Tsui, “Nobel lecture: Interplay of disorder and interaction in two-dimensional electron gas in intense magnetic fields,” *Rev. Mod. Phys.*, vol. 71, pp. 891–895, Jul 1999.
- [9] K. v. Klitzing, G. Dorda, and M. Pepper, “New method for high-accuracy determination of the fine-structure constant based on quantized hall resistance,” *Phys. Rev. Lett.*, vol. 45, pp. 494–497, Aug 1980.
- [10] D. C. Tsui, H. L. Stormer, and A. C. Gossard, “Two-dimensional magnetotransport in the extreme quantum limit,” *Phys. Rev. Lett.*, vol. 48, pp. 1559–1562, May 1982.
- [11] J. J. Sakurai, *Meccanica quantistica moderna*. Zanichelli, 1996.
- [12] L. D. Landau and E. M. Lifshits, *Fisica Teorica 3 - Meccanica quantistica*. Editori riuniti, 2010.
- [13] F. Herlach and N. Miura, eds., *High Magnetic Fields. Science and Technology. Volume 2: Theory and Experiments I*. World Scientific, 2003.
- [14] R. B. Laughlin, “Quantized hall conductivity in two dimensions,” *Phys. Rev. B*, vol. 23, pp. 5632–5633, May 1981.
- [15] H. Aoki and T. Ando, “Effect of localization on the hall conductivity in the two-dimensional system in strong magnetic fields,” *Solid State Communications*, vol. 38, no. 11, pp. 1079 – 1082, 1981.
- [16] P. Fulde, *Correlated Electrons in Quantum Matter*. World Scientific, 2012.
- [17] E. J. Bergholtz and A. Karlhede, “Quantum hall system in tao-thouless limit,” *Phys. Rev. B*, vol. 77, p. 155308, Apr 2008.
- [18] P. Bak and R. Bruinsma, “One-dimensional ising model and the complete devil’s staircase,” *Phys. Rev. Lett.*, vol. 49, pp. 249–251, Jul 1982.

-
- [19] K. Huang, *Statistical Mechanics, Second Edition*. Wiley, 1987.
- [20] R. K. Pathria and P. D. Beale, *Statistical Mechanics, Third Edition*. Academic Press, 2011.
- [21] L. Peliti, *Statistical Mechanics in a Nutshell*. Princeton Univ Pr, 2011.
- [22] T. D. Lee and C. N. Yang, “Statistical theory of equations of state and phase transitions. ii. lattice gas and ising model,” *Phys. Rev.*, vol. 87, pp. 410–419, Aug 1952.
- [23] M. Bundaru, N. Angelescu, and G. Nenciu, “On the ground state of ising chains with finite range interactions,” *Physics Letters A*, vol. 43, no. 1, pp. 5 – 6, 1973.
- [24] S. Aubry, “Exact models with a complete devil’s staircase,” *Journal of Physics C: Solid State Physics*, vol. 16, no. 13, p. 2497, 1983.
- [25] V. L. Pokrovsky and G. V. Uimin, “On the properties of monolayers of adsorbed atoms,” *Journal of Physics C: Solid State Physics*, vol. 11, no. 16, p. 3535, 1978.
- [26] E. Levi, J. Minár, and I. Lesanovsky, “Commensurate-incommensurate transitions in a one-dimensional two-component lattice gas with $1/r^\alpha$ interactions.” arXiv:1503.03268.
- [27] P. Bak and J. von Boehm, “Ising model with solitons, phasons, and ”the devil’s staircase”,” *Phys. Rev. B*, vol. 21, pp. 5297–5308, Jun 1980.
- [28] S. E. Burkov and Y. G. Sinai, “Phase diagrams of one-dimensional lattice models with long-range antiferromagnetic interaction,” *Russian Mathematical Surveys*, vol. 38, no. 4, p. 235, 1983.